VirID: Beyond Virus Discovery - An Integrated Platform for Comprehensive RNA Virus Characterization

Ziyue Yang[#,1,2,3], Yongtao Shan[#,1,2,3], Xue Liu[1,2,3], Guowei Chen[4], Yuanfei Pan[5], Qinyu Gou[1,2,3], Jie Zou[1,2,3], Zilong Chang[1,2,3], Qiang Zeng[1,2,3], Chunhui Yang[1,2,3], Jianbin Kong[1,2,3], Yanni Sun[4], Shaochuan Li[6], Xu Zhang[6], Wei Chen Wu[1,2,3], Chunmei Li [1,2,3], Hong Peng[1,2,3], Edward C. Holmes[7,8], Deyin Guo*[9,10], Mang Shi*[1,2,3,11]

[1]State Key Laboratory for Biocontrol, School of Medicine, Shenzhen Campus of Sun Yat-sen University, Sun Yat-sen University, Shenzhen, China.

[2]National Key Laboratory of Intelligent Tracking and Forecasting for Infectious Diseases, Sun Yat-sen University, Shenzhen, China.

[3]Shenzhen Key Laboratory for Systems Medicine in Inflammatory Diseases, Shenzhen Campus of Sun Yat-sen University, Sun Yat-sen University, Shenzhen, China.

[4]Department of Electrical Engineering, City University of Hong Kong, 83 Tat Chee Avenue, Kowloon, Hong Kong (SAR), China.

[5]Ministry of Education Key Laboratory of Biodiversity Science and Ecological Engineering, School of Life Sciences, Fudan University, Shanghai, China.

[6]Goodwill Institute of Life Sciences, Guangzhou, China.

[7]School of Medical Sciences, The University of Sydney, Sydney, New South Wales, Australia.

[8]Laboratory of Data Discovery for Health Limited, Hong Kong SAR, China.

[9]Guangzhou National Laboratory, Guangzhou International Bio-Island, Guangzhou, China.

[10]State Key Laboratory of Respiratory Disease, National Clinical Research Center for Respiratory Disease, Guangzhou Institute of Respiratory Health, The First Affiliated Hospital of Guangzhou Medical University, Guangzhou, Guangdong, China.

[11]Guangdong Provincial Center for Disease Control and Prevention, Guangzhou, China.

[#]These authors contributed equally to this work

*Corresponding authors: De-yin Guo (Email: guodeyin@mail.sysu.edu.cn) and Mang Shi (shim23@mail.sysu.edu.cn)

Abstract

RNA viruses exhibit vast phylogenetic diversity and can significantly impact public health and agriculture. However, current bioinformatics tools for viral discovery from metagenomic data frequently generate false positive virus results, overestimate viral diversity, and misclassify virus sequences. Additionally, current tools often fail to determine virus-host associations, which hampers investigation of the potential threat posed by a newly detected virus. To address these issues we developed VirID, a software tool specifically designed for the discovery and characterization of RNA viruses from metagenomic data. The basis of VirID is a comprehensive RNA-dependent RNA polymerase (RdRP) database to enhance a workflow that includes RNA virus discovery, phylogenetic analysis, and phylogeny-based virus characterization. Benchmark tests on a simulated data set demonstrated that VirID had high accuracy in profiling viruses and estimating viral richness. In evaluations with real-world samples, VirID was able to identity RNA viruses of all type, but also provided accurate estimations of viral genetic diversity and virus classification, as well as comprehensive insights into virus associations with humans, animals, and plants. VirID therefore offers a robust tool for virus discovery and serves as a valuable resource in basic virological studies, pathogen surveillance, and early warning systems for infectious disease outbreaks.

Keywords

RNA virus; Virus discovery; Phylogenetic analysis; Virome; Emerging pathogens

Introduction

RNA viruses are renowned for their genetic and phenotypic diversity and ability to infect hosts ranging from animals, plants, fungi, to microbial organisms, sometimes with devastating health and economic consequences (Nicaise 2014). RNA viruses have caused human epidemics for millennia, with notable recent examples including human immunodeficiency virus (HIV; 1981) (Fauci 1988), SARS-CoV (2002) (Zhong, et al. 2003), pandemic H1N1 influenza (2009) (Smith, et al. 2009), MERS-CoV (2012) (Assiri, et al. 2013), Ebola virus (Western Africa, 2013) (Team 2014), Zika virus (2015) (Musso and Gubler 2016) and most recently SARS-CoV-2 (2019) (Zhu, et al. 2020). Importantly, approximately 70% of these pandemic-causing viral pathogens originate from wildlife animals or utilize arthropod vectors (Chan, et al. 2013), and many evaded surveillance systems before their emergence in human populations (Claas, et al. 1998; Ergönül 2006; Peiris, et al. 2007; Martina, et al. 2009). Additionally, RNA viruses pose significant threats to agriculture, particularly as epidemics in domestic animals and crops can jeopardize global food security (Mackenzie, et al. 2004; Untiveros, et al. 2007; Scholthof, et al. 2011; Lee 2015; Robilotti, et al. 2015; He and Krainer 2020). Understanding the diversity of RNA viruses and enhancing surveillance of those that pose threats to humans and economically important species are therefore endeavors of utmost importance (Carroll, et al. 2018; Lefrançois, et al. 2023).

Meta-transcriptomics (i.e., total RNA sequencing) provides a potentially unbiased survey of the genetic information from all types of organisms in biological samples and has transformed the detection and characterization of RNA viruses (Simmonds, et al. 2017; Greninger 2018; Shi, Lin, et al. 2018; Shi, Zhang, et al. 2018; Zhang, et al. 2019). This method provides efficiency and breadth in virus discovery compared to traditional cultivation techniques (Shi, et al. 2016; Chen, et al. 2022; Zayed, et al. 2022), which are often restricted by their reliance on cell culture growth (Huhtamo, et al. 2012; Shi, Lin, et al. 2018), and to PCR-based approaches that depend on prior knowledge of existing viral diversity (Culley, et al. 2003). As a consequence, meta-transcriptomics has become the primary tool for discovering RNA viruses (Greninger 2018), with the highly conserved RNA-dependent RNA polymerase (RdRP) that is essential for RNA virus replication serving a powerful universal genetic marker

(Holmes 2009; Li, Shi, et al. 2015; Lam, et al. 2020; Edgar, et al. 2022; Mifsud, et al. 2022; Shi, et al. 2023).

As well as sequencing, the bioinformatics tools for detecting and characterizing virus sequences within metagenomic data sets have experienced major improvements. Initial workflow tools like ViromeScan (Rampelli, et al. 2016) and Taxonomer (Flygare, et al. 2016) detected viruses in samples by analyzing sequencing reads. Subsequent tools, such as Vipie (Lin, et al. 2017), ID-seq (Kalantar, et al. 2020), Lazypipe2 (Plyusnin, et al. 2023), and ViWrap (Zhou, et al. 2023), use contigs from *de novo* assemblies for virus identification, enhancing the length of query sequences and aiding the discovery of divergent viruses. With the advent of machine learning and deep learning, tools such as PhiSpy (Akhter, et al. 2012), VirSorter (Roux, et al. 2015), VirSorter2 (Guo, et al. 2021), and VIBRANT (Kieft, et al. 2020) were developed to differentiate viral from microbial sequences by analyzing gene and/or genomic sequences and features. Furthermore, methods like VirFinder (Ren, et al. 2017) and DeepVirFinder (Ren, et al. 2020) utilize the frequency of consecutive nucleotides (k-mers) in known viral and cellular genomes to identify DNA bacteriophage. More recently, specialized RNA virus discovery software such as VirBot (Chen, Tang, et al. 2023) have been developed. VirBot constructs databases of RNA virus protein families and employs profile Hidden Markov Models (pHMM) to identify distantly related viral sequences, exhibiting superior performance to other virus classification tools.

Despite these advancements, the bioinformatics tools for virus discovery continue to confront major challenges, such as a high false positive rate, the overestimation of viral diversity, and inaccurate virus classification (Dutilh, et al. 2021; Hegarty, et al. 2024). These issues are particularly problematic for RNA viruses due to their highly divergent genomes and distinct genomic structures which complicate identification using basic annotation methods (Drake 1993; Simon-Loriere and Holmes 2011). Additionally, current bioinformatics tools often lack the capability for the in-depth characterization of viruses, including the accurate identification of host associations, which impedes an understanding of their potential threat to public health and agricultural systems.

In response to these challenges, we developed VirID – a comprehensive and user-friendly

software tool tailored for the discovery and characterization of RNA viruses from metagenomic data. VirID features a robust database of RdRP sequences and comprises three core modules: (i) RNA virus discovery, (ii) phylogenetic analysis, and (iii) phylogeny-based virus characterization. Benchmark tests on simulated data set revealed VirID's high accuracy in profiling and classifying RNA viruses. In practical applications with real-world data sets, VirID demonstrated its capacity for virus discovery and for conducting thorough virome analyses.

Materials and Methods

RdRP Database

We established a database of 7080 representative RdRP protein sequences for RNA virus discovery and characterization. The RdRP sequences were derived from three independent sources, including a "backbone RdRP data set" (N = 5,384) (Shi, et al. 2016; Shi, Lin, et al. 2018), the NCBI RefSeq database (viral RdRP associated, N = 19,574), and the NCBI GenBank database (viral RdRP associated, N = 5,710,331). RdRPs from the RefSeq and GenBank databases were initially identified based on key annotation terms, including "RdRP", "RNA-dependent RNA polymerase" and "polymerase" under the taxonomy "Riboviria". Highly divergent RdRPs derived from environmental samples (Edgar, et al. 2022; Zayed, et al. 2022; Hou, et al. 2023) were excluded due to lack of confirmation. The RdRPs from NCBI were then compared to the backbone RdRP data set using Diamond v2.1.4 (Buchfink, et al. 2015), with an e-value threshold of 1e-5 and the '--ultra-sensitive' parameter, and sequences with BLAST hit results were retained. The presence of key RdRP domains, specifically the highly conserved A, B and C sequence motifs, were examined using palmscan v1.0.i86linux64 (Babaian and Edgar 2022). The remaining sequences were clustered using CD-HIT v4.8.1 (Fu, et al. 2012) at 80% amino acid identity, with a representative then selected from each cluster. CD-HIT's default parameters chose the longest sequences, which were then reviewed and corrected for any errors. This resulted in a final reference database of 7080 sequences that were then systematically organized into 24 RNA virus "superclades" based on broad phylogenetic relationships (Figure 1A)(Shi, et al. 2016; Shi, Lin, et al. 2018), and subsequently into 5 phyla, 20 classes, 28 orders, and 112 families based on both the phylogenetic relationships and ICTV taxonomy (Figure 1B, Supplementary Table S1).

139 For each of the RdRP sequences, information on host organism was initially retrieved from
140 the Virus-Host Database (Mihara, et al. 2016) and confirmed by checking the original
141 publications. Based on the host information and phylogenetic relationships, we categorized the
142 RdRP sequences into four broad groups: (i) those infecting humans (including vector-borne
143 viruses, N = 188), (ii) those infecting vertebrate animals (N =363), (ii) those infecting plants
144 (N = 325), and (iv) all other host associations (Figure 1C). This information, together with virus
145 phylogenetic relationships, was used to define specific host groups on phylogenetic trees
146 (Figure 1D, Supplementary Figure S1) from which the host-association of the newly identified
147 RdRP sequences could be inferred (See below).
148
149 **Processing and Assembly of Sequencing Reads**
150 VirID performs an initial processing of the input read sequences. The quality control of
151 reads was conducted using bbduk.sh (Bushnell 2014). To remove host and microbial ribosomal
152 RNA (rRNA) sequences, the reads were then mapped, using Bowtie2 v 2.5.1 (Langmead and
153 Salzberg 2012), against a reference rRNA database that contained a total of 505,405 rRNA non-
154 repetitive sequences obtained from SILVA database v138.1 (Quast, et al. 2012) and the RDP-
155 II database (Cole, et al. 2007). The remaining reads were assembled *de novo* into contigs using
156 MEGAHIT v1.2.9 (Li, Liu, et al. 2015) and under default parameters. Only contigs longer than
157 600bp were retained for subsequent virus discovery and characterization.
158
159 **Discovery and Quality Control of RNA Virus Contigs**
160 VirID discovers RNA viral contigs through a homology-based search approach. The
161 assembled contigs were first compared against the RdRP reference database using the Diamond
162 BLASTx program v2.1.4 with the e-value threshold of 1e−4 to identify potential RNA viral
163 sequences. To remove false positives, potential viral contigs were subsequently compared
164 against the NCBI Non-Redundant Protein Database (NR) with the e-value threshold of 1e−4
165 and the hits were annotated using TaxonKit v0.14.2 (Shen and Ren 2021). Contigs with only
166 non-viral hits were removed, and the top hits of the remaining contigs were used to provide an
167 initial taxonomic annotation for the viral contigs.

168 In addition to the standard quality control steps described above, VirID employs extra
169 procedures to identify and remove false positives and erroneous sequences. To filter out
170 potential endogenous virus elements (EVEs) with disrupted ORFs, we removed contigs whose
171 RdRP-associated open reading frames (ORFs) were predicted to contain less than 200 amino
172 acids by scanning the viral sequence in six possible reading frames. For ORF prediction, we
173 included an option for 26 genetic code sets available in the NCBI database, with the standard
174 code set as the default. To identify and control for misassembled contigs that contained both
175 viral and non-viral sequences, the sequence was first compared using BLASTn (Camacho, et
176 al. 2009) against a "non-viral" database, specifically a sub-set of NCBI Nucleotide Sequence
177 Database (NT) that excludes viral sequences. Based on the position and length of hit, the target
178 contigs were either partially corrected (i.e., in scenarios when "non-viral" regions appeared at
179 either end of the contigs and were shorter than the "viral" region) or completely removed (all
180 other cases).
181
182 **RNA Virus Species Identification and Quantification**
183 For viral species identification, the RdRP-associated contigs were clustered using the all-
184 to-all BLASTn method (Nayfach, et al. 2021), employing an 80% sequence identity and a 40%
185 sequence length threshold to define approximate species-level taxonomic units. For each
186 species-level group, the predicted RdRPs were compared against the NR database, and those
187 with >90% identity and 70% coverage to existing RNA viral species were denoted "known"
188 viral species, whereas those below these thresholds were considered as "new" viral species.
189 The sequence Reads Per Million (RPM) metric was used to evaluate the relative abundance
190 of virus species within the sample. Clean reads are first mapped to all contigs associated with
191 a virus species using Bowtie2 v2.5.1(Langmead and Salzberg 2012). The number of mapped
192 reads is multiplied by 10^6 and divided by the total number of reads to give the RPM value.
193 $$RPM = \frac{MappedReads * 10^6}{TotalReads}$$
194
195 **Viral Sequence Alignment at the Superclade Level**
196 For newly identified viral sequences, multiple alignment was performed before subsequent

197 phylogenetic placement. Viral RdRP sequences were first classified into 24 superclades for
198 sequence alignment and phylogenetic analysis, based on BLASTx comparisons (Camacho, et
199 al. 2009) against the RdRP reference database. To accelerate the analysis of the Picorna-Calici
200 superclade, we excluded contigs encoding proteins with fewer than 400 amino acids before
201 alignment. This was necessary due to the Picorna-Calici superclade containing 533 reference
202 sequences, which made each alignment iteration time-consuming. VirID utilizes the Amino
203 Acid Consistency (AAC) index to quantify the similarity between two aligned amino acid
204 sequences. AAC is calculated by dividing the number of identical amino acids (excluding gaps)
205 by the total length of the aligned amino acid sequence.

206 To ensure the accuracy of multiple sequence alignments, we employed an iterative
207 approach with Mafft v7.520 (Katoh and Standley 2013), followed by the removal of
208 ambiguously aligned regions using trimAl v1.4 (Capella-Gutiérrez, et al. 2009). In each
209 iteration, for each reference sequence (R^i), its amino acid identity r^i is determined by the
210 highest amino acid identity value compared to other reference sequences. For each potential
211 viral sequence (Q^i), its amino acid identity q^i is set as the maximum value when compared
212 to all reference sequences. If q^i falls below the minimum value of R across the entire reference
213 sequence set, the sequence Q^i is removed as a poor-quality sequence, and the alignment
214 process is repeated. The pseudocode for eliminating false positives through multiple sequence
215 alignment is provided in Supplementary Figure S2.

216 $$r^i = \max_{i \neq j} AAC(R^i, R^j)$$

217 $$q^i = \max_{k \in RefList} AAC(Q^i, R^K)$$

218

219 **Phylogenetic Placement**

220 To optimize phylogenetic tree inference, we implemented an approach based on reference
221 trees. We first estimated reference maximum likelihood trees in RaxML v7 (Stamatakis, et al.
222 2008), using the best fit amino acid substitution model (i.e., PROTGAMMALGF) selected by
223 ProtTest (Abascal, et al. 2005). Subsequently, new sequences were integrated into these pre-
224 built reference trees based on the alignment using the LG model in pplacer v1.1 (Matsen, et al.
225 2010), which accurately identifies their most likely topological positions. The output from

226 pplacer, provided in JSON format, is then converted into the Newick tree format using guppy
227 v1.1 (Matsen, et al. 2010), facilitating further phylogenetic analyses.
228 To evaluate the reliability of our phylogenetic placement, we performed leave-one-out
229 cross-validation, focusing on tree recall, which measures the proportion of correctly recovered
230 branches. For this analysis, we only included branches supported by a bootstrap confidence
231 value exceeding 90%. We observed that the distribution of recall rates varied across superclades,
232 likely influenced by the number of reference sequences and their similarity. In superclades
233 containing more than 50 sequences, recall rates for most clades tended to concentrate around
234 0.75, with few deviations (Supplementary Figure S3). Additionally, in virus clades with a high
235 density of sequences, such as Picorna-Calici and Partiti-Picobirna, this placement method
236 maintained the fundamental stability of the tree structure, demonstrating robustness despite the
237 addition of numerous new sequences.
238
239 $$Tree\ recall = \frac{Edge_{both}}{Edge_{\text{reference}}}$$
240
241 **Classification and Host Association Inference Based on Phylogenetic Analysis**
242 The classification and host association of a query genome were inferred based on its
243 placement within each RdRP superclade tree. We systematically annotated the evolutionary
244 tree by traversing from the leaf nodes upwards, adhering to the principle that sibling nodes
245 share the same labels. The labeling process for each leaf node followed the following criteria:
246 (i) if the node corresponds to a known sequence, its label is assigned based on the existing
247 annotation; (ii) if its sibling node is a known sequence, the leaf node inherits the label of its
248 sibling; and (iii) if its sibling node is an internal node, we iteratively determined the label of
249 that internal node before assigning it to the leaf node. For internal nodes, we conducted a
250 systematic top-down traversal of all their daughter nodes. If all daughter nodes carry identical
251 labels, the internal node adopts the same label as its descendants. However, if the daughter
252 nodes have differing labels, the internal node is categorized under the lowest common
253 taxonomic label for all those leaf nodes in this superclade. This structured approach ensures
254 consistent and logical assignment of labels throughout each superclade tree.

255 Each potential viral sequence is assigned two types of labels: a taxonomic label that spans
256 superclade-taxon to ICTV hierarchical classification and eventually down to the species level,
257 and a host association label that categorizes the virus as related to humans, vertebrates, or plants.
258 During the phylogenetic tree annotation, host association tags (represented as 0 or 1) are
259 assigned to sequences. Specifically, if a viral sequence's sibling node is identified as a human
260 pathogen, the sequence is considered potentially relevant to humans only if the similarity
261 exceeds 80%. For the ICTV classification within the phylogenetic tree, each internal node is
262 labeled according to the lowest common taxonomic level of its descendant nodes. For
263 sequences that remain unclassified, a default taxonomic hierarchy is assigned within the
264 corresponding superclade. This classification system effectively categorizes potential viral
265 sequences up to the genus level. For well-documented viruses, species-level classification is
266 determined using the NCBI annotation file derived from comparisons within the NR database.
267 This rigorous approach ensures accurate and detailed categorization of viral sequences across
268 various levels of taxonomic and host associations.
269
270 **Benchmarking Preliminary Viral Contig Screening on Simulated Data Set**
271 To evaluate the performance of VirID in the preliminary screening of RNA viral sequences,
272 we constructed a simulated short-read shotgun metagenomic data set for benchmarking using
273 CAMISIM (Fritz, et al. 2019). This data set included 15 samples from three categories: 'known
274 RNA viruses', 'new RNA viruses', and 'others', with each category comprising 15 species. The
275 'known RNA viruses' and 'others' data sets were derived from 463 complete RNA virus
276 genomes and 55 complete non-RNA virus genomes available in the NCBI RefSeq database,
277 respectively (Supplementary Figure S4). The 'new RNA viruses' were subdivided into three
278 levels based on their sequence similarity to the reference database and containing five species
279 each: 'new RNA virus L1', 'new RNA virus L2', and 'new RNA virus L3', with similarity
280 thresholds set at $0.70 \leq$ similarity (L1) ≤ 0.90, $0.40 \leq$ similarity (L2) < 0.70, and $0.20 \leq$
281 similarity (L3) < 0.40, respectively. The sequences used to simulate 'new RNA viruses' were
282 sourced from 299 high-quality RNA virus sequences obtained from recent publications (Feng,

et al. 2022; Cui, et al. 2023; Hou, et al. 2023; Wang, et al. 2023), ensuring a comprehensive and challenging test environment.

The individual simulated data samples are provided in pair-end fastq format, with each file approximately 20 GB in size and each read 150 base pairs long. The distribution of the three data types within each sample is maintained at a consistent ratio of 1:1:1. Unlike other tools that require contigs, VirID accepts reads directly as input. To ensure consistent data standards across all tools, the contigs generated from VirID's intermediate outputs are used as input for the other tools. Additionally, for uniformity in evaluation metrics, all tools have adopted VirID's criterion of using contigs longer than 600bp.

We assessed the performance of three different RNA viral detection tools—VirSorter2, VirBot, and VirID—on a simulated data set using accuracy, precision, recall, and F1 score. These metrics focus on the number of correctly identified species in the tool's output, rather than the number of sequences. The accuracy of each tool reflects the proportion of RNA viral species correctly identified from the total number of species. Recall measures the tool's sensitivity by calculating the proportion of RNA viral species detected relative to the total number of RNA viral species in the data set. Precision indicates the specificity of the tool, defined as the proportion of RNA viral species detected out of the total number of species identified by the tool. The F1 score, the harmonic mean of precision and recall, provides a balanced measure of a tool's overall effectiveness.

Metagenomic Data Sets

To demonstrate VirID's visualization capabilities, we analyzed 20 SRA libraries from a large scale animal study conducted in China (Cui, et al. 2023) that comprised 14 animal species across five provinces. In addition, we assessed the versatility of VirID through the analysis of 192 public libraries from seven studies, which included a wide range of samples from human swabs (Graf, et al. 2016) and diverse animal tissues (Chang, et al. 2020; He, Wang, et al. 2022; Shi, et al. 2022), as well as arthropod (Pettersson, et al. 2020), plant (Elmore, et al. 2022), and soil samples (Bender, et al. 2021). The public metagenomes utilized in this analysis were sourced from NCBI, with details provided in Supplementary Table S2, S3.

312

313 **Benchmark on Real Metagenomics Data Set**

314 To evaluate the performance of VirID and VirBot for real-world data sets, we conducted a
315 benchmark analysis using 20 wildlife sequencing libraries (Supplementary Table S2). VirBot
316 utilized intermediate assembled contigs from VirID as input. For the contigs identified by VirID
317 and VirBot, ORFs were translated using standard genetic code and annotated based on aligning
318 predicted amino acid sequences to hidden Markov models (HMMs) from the Pfam-A database
319 (https://pfam-legacy.xfam.org/) using HMMER's hmmscan (http://hmmer.org/), with a
320 minimum score threshold of 25. ORFs without hits in Pfam-A were further annotated using
321 BLASTp against the NR protein database with an e-value threshold of 1e-4. We then
322 categorized the top hit annotations of ORFs into three groups: (i) those contained RdRP protein,
323 and those did not contain RdRP, but contained (ii) non-structural proteins other than RdRP, and
324 (iii) structural proteins. To further compare the taxonomic classification performance of VirID
325 and VirBot, we compared the classifications of contigs identified by VirID. We calculated the
326 percentage of sequences classified at each of the seven taxonomic levels, from realm to genus.

327 We benchmarked the runtime of VirID, VirBot, and VirSorter2 using 5 real-world
328 sequencing samples with sequencing data size ranging from 2.6GB to 15.8GB (see
329 Supplementary Table S4 for details). All runtime estimations were conducted in an
330 environment running Ubuntu 22.04.2 LTS (GNU/Linux 5.15.0-116-generic x86_64) with four
331 AMD EPYC 7643 48-core processors and 1.0 TB of memory. The programs were restricted to
332 32 threads, with no memory limitations. VirID used sequencing reads in '.fastq.gz' format as
333 input, while VirBot and VirSorter2 used intermediate assembled contigs from VirID,
334 comprising sequences longer than 300 bp. To ensure a fair comparison, we used contigs as the
335 starting material when performing comparisons among the three methods. Additionally, we
336 estimated the computational runtime for the unique steps in the VirID analysis pipeline,
337 including (i) read assembly and (ii) phylogenetic inference, recognizing that these steps could
338 not be directly compared with the other methods due to the absence of equivalent processes.

339

340 **Parameters and Visualizations**

341 VirID offers three user-selectable modes: 'end to end', 'assembly and basic annotation', and
342 'phylogenetic analysis'. The 'end to end' mode executes both 'assembly and basic annotation'
343 and 'phylogenetic analysis' sequentially. The 'assembly and basic annotation' mode processes
344 sequencing data up to the point of producing annotated contigs, but it does not include
345 phylogenetic analyses. Conversely, the 'phylogenetic analysis' mode begins with contigs and
346 carries out subsequent processing from there.

347 During the 'assembly and basic annotation' stage, users can opt to remove mis-assembled
348 portion of a virus contig, a process that may require longer time and significant memory
349 resources. Additionally, an ultrasensitive mode is available for analyzing RdRP libraries that
350 enhances the detection of a broader range of potential viral sequences. In the 'phylogenetic
351 analysis' phase, users can choose to eliminate redundant sequences and customize the amino
352 acid length thresholds for specific superclade of interest. VirID employs several tools for
353 visualizations: sankey diagrams, stacked histograms, and phylogenetic tree diagrams are
354 generated using the R packages networkD3 (Allaire, et al. 2017), ggtree (Yu, et al. 2017), and
355 ggplot2 (Wickham 2011), respectively. Further visualizations are created using Matplotlib
356 v3.7.4 (Hunter 2007) and Seaborn v0.13.0 (Waskom 2021), enabling comprehensive graphical
357 representations of the data.

358

359 **Results**

360 **VirID Workflow**

361 VirID is a user-friendly command-line tool designed for the detection and detailed
362 characterization of RNA viruses from metagenomic data. The workflow is divided into three
363 stages: RNA virus discovery, phylogenetic analysis, and phylogeny-based virus
364 characterization (Figure 2). In the first stage, putative RNA virus genomes containing the RdRP
365 gene are identified through a homology approach, checked for false positives and
366 contamination, and clustered based on sequence similarity at the species level. This process
367 yields high-quality genomic sequences and related information such as sequence length, closest
368 relatives, and abundance levels. In the second stage, VirID conducts high-quality sequence
369 alignment and comprehensive evolutionary analysis across the full diversity of the RNA

370 virosphere: this further removes low-quality sequences and reveals the phylogenetic position
371 of all newly discovered viruses. In the final stage, based on these evolutionary analyses, VirID
372 provides precise classification information and predicts potential viral associations with
373 humans, vertebrates, and plants.
374
375 **Analysis Results Output in VirID**
376 VirID conducts thorough data analyses and offers robust visualization tools, enabling an
377 intuitive and comprehensive presentation of results. VirID organizes its output into three main
378 folders: (i) 'assembly and basic annotation' for intermediate files related to RNA virus
379 discovery, (ii) 'phylogenetic analysis' containing well-labelled trees for various superclades,
380 and (iii) 'results' for other figures and tables. It generates tables, fasta format sequences files,
381 web files, and figure files (pdf format) to suit various analytical needs. We demonstrated these
382 features here using a data set from 20 wildlife sequencing libraries that includes bats,
383 insectivores, pangolins, pika and rodent samples (Cui, et al. 2023) (Figure 3, Supplementary
384 Table S2). In the RNA virus discovery segment, VirID estimates Reads Per Million (RPM)
385 values for each potential viral species to assess their relative abundance. These values are
386 displayed in a sankey plot on an HTML webpage, illustrating RPM distributions across RdRP
387 superclades and NCBI taxonomy at multiple taxonomy levels—phylum, class, order, family,
388 genus, and species (Figure 3A). VirID also categorizes potential viral sequences into one or
389 two of four host-association groups: human, vertebrate, plants, and others (Figure 3B). This
390 information is provided in color-coded trees that contain information on both phylogenetic
391 relationships and potential host associations (Figure 3C). Additionally, VirID outputs high-
392 quality viral genome sequences in fasta format (Figure 3D) and all other relevant information,
393 including sequence length, highest BLASTx match, virus classification, association with
394 principal hosts, in multidimensional tables (Figure 3E, Supplementary Table S5, S6).
395 In the example of the 20 wildlife sequencing libraries VirID identified 129 potential RNA
396 viral contigs belonging to 107 various species, including 87 new virus species, spanning 26
397 families and 15 superclades (Supplementary Figure S5A). Overall, 54 of these species can be
398 assigned at the family level, with the remainder falling outside known families. Eleven of these

399 species are potentially relevant to humans, including Wufeng Niviventer niviventer
400 orthohantavirus 1, Severe acute respiratory syndrome-related coronavirus, Rotavirus A, and
401 Pangolin respirovirus (Supplementary Figure S5B, Supplementary Figure S6). Additionally,
402 several viral species associated with vertebrate infections were identified, including those
403 within the genera *Alphacoronavirus*, *Alphainfluenzavirus*, and *Mammarenavirus*. The
404 remaining 88 viral species are most likely derived from diet, parasites, and other microbial
405 cellular organisms within the principal host, because they were identified as plant viruses (e.g.
406 members of the *Tombunsviridae*) or closely related to arthropod (e.g. *Iflaviridae*) or fungal
407 viruses (e.g. *Mitoviridae*).
408
409 **Benchmarking VirID using Simulated Data**
410 We initially evaluated VirID alongside two other tools—VirSorter2, VirBot—using a
411 collection of simulated samples (N = 15) that included a diverse mix of RNA viruses and other
412 species. These read data samples were generated using the CAMISIM simulator, drawing on
413 source genomes and sequences from both the NCBI RefSeq database and recent studies. The
414 RNA viruses in the CAMISIM pool were comprised of four categories: 'known RNA viruses',
415 'new RNA virus L1', 'new RNA virus L2', and 'new RNA virus L3', representing different
416 similarity levels to the reference database sequences.
417 Three tools were compared across 15 data samples, including the average accuracy,
418 precision, recall, and F1 score metrics (Figure 4A). VirID achieved the highest F1 score of
419 0.9334, with a standard error of ±0.0180. Its recall, at 0.8822 with a standard error of ±0.0301,
420 was close to VirBot (0.8822 ± 0.0247). Notably, VirID's precision was perfect across all 15
421 samples, with an absence of false positives. The three tools were further evaluated for their
422 performance on 'new RNA viruses' that shared less than 90% amino acid identity with those
423 described in NCBI database (Figure 4B) and 'known RNA viruses'. VirID continued to perform
424 well in identifying 'new RNA viruses', again with zero false positives (Supplementary Figure
425 S7).
426 We also analyzed whether the number of viral sequences or species revealed by each tool
427 matched that of expected species count in the simulated data (Figure 4C). VirID's estimation

428 of contigs (39, average) and species (27, average) were the most closely aligned with the 30
429 true species samples, followed by VirSorter2 (average of 45 contigs and 26 species) and then
430 VirBot (53 contigs and 27 species). VirID achieved a ratio of 1.47 for the number of estimated
431 sequences relative to the number of true species. This ratio was the lowest among all tools,
432 indicating that VirID's output most accurately reflect the actual number of virus species.

433 The integrity of the RNA viral sequences revealed and processed by VirID was assessed
434 using the CAMISIM simulator's 'gold standard' contigs as a benchmark. These standard contigs
435 represent idealized assembly results of the simulated reads, providing a baseline for evaluating
436 the detected virus sequences. We aligned the putative viral contigs with these 'gold standard'
437 contigs, selecting the best matches based on coverage and identity. The average completeness
438 for contigs in 10 samples exceeded 90%, with an overall average completeness of 90.80%
439 across all 15 samples (Figure 4D). This meets CheckV's criterion for 'high quality
440 completeness' (Nayfach, et al. 2021).

441

442 **Benchmarking VirID on Real-world Sequencing Libraries**

443 We conducted a benchmark analysis of the VirID and VirBot RNA discovery tools using
444 the 20 wildlife sequencing libraries described above (Supplementary Figure S8). VirID and
445 VirBot both identified 212 contigs (Supplementary Figure S8A). VirBot detected an additional
446 438 unique contigs, of which 240 were short contigs (<200 amino acids) and the remainder
447 primarily encoded non-RdRp proteins. In contrast, VirID identified 23 additional contigs, all
448 of which encoded RdRPs (Supplementary Figure S8B). This suggests that VirBot identifies
449 more viral contigs overall, while VirID gives a more accurate representation of viral richness.
450 Additionally, we compared the percentage of annotated contigs from the final 129 contigs
451 obtained by VirID. Since VirID uses phylogenetic analysis for classification, it achieved more
452 detailed viral classification across various taxonomic levels (Supplementary Figure S8C).

453 In regard to computational runtime estimation based on 32 threads of the AMD EPYC
454 7643 CPU, VirID (median 15.7 minutes, 11.3 - 28.4 minutes) and VirBot (median 5.2 minutes,
455 1 - 14.1 minutes) demonstrated similar performance, while VirSorter2 (median 141.9 minutes,
456 3.4 - 216.8 minutes) was significantly slower (Supplementary Figure S8E). For the unique steps

457 in VirID, read assembly took a median of 92.5 minutes (4.5 – 126.2 minutes), with runtime
458 positively correlated with the sequencing depth of the sample (Supplementary Figure S8D).
459 Phylogenetic inference had a median runtime of 1.3 hours (0.3 – 16.9 hours), with the longest
460 time spent on sequence alignment (Supplementary Figure S8F). The longest runtimes (16.3
461 and 16.9 hours) were observed in data sets containing members of the Picorna-Calici clade,
462 which included a total of 533 reference viral sequences. The CPU runtime for phylogenetic
463 inference could be significantly reduced by improving the speed of sequence alignment.
464

465 **A Re-Analyses of Previously Published Data Sets**

466 We next assessed the performance of VirID by analyzing 192 meta-transcriptomic SRA
467 libraries from seven distinct virome studies, covering a range of sample types including clinical
468 (human), wild birds, Malayan pangolins, Qinghai voles, seabird ticks (*Ixodes uriae*), soybean
469 fields, and peat soil samples (Supplementary Table S3). VirID significantly improved viral
470 discovery. A total of 1,283 RNA viral species were identified in these data sets, with the soil
471 samples displaying the highest average virus species richness at 88.5 species per sample,
472 followed by Qinghai vole at 2, and then seabird tick at 1.9. Importantly, 1,202 novel RNA viral
473 species were identified. Among these, the highest number of novel viruses ($N = 740$) was found
474 in the soil samples, with 56% of these viruses categorized within the Narna-Levi superclade.
475 At the family level, the *Picobirnaviridae* contained the most viral species ($N = 164$), followed
476 by the *Tombusviridae* ($N = 83$) and *Mitoviridae* ($N = 69$), although many virus species (54.5%)
477 could not be assigned at family level (Figure 5A).

478 We next evaluated the number of families identified and compared these with previous
479 studies, omitting any with incomplete classification information. Our analysis revealed an
480 average increase of five viral families, with notable differences particularly observed in the
481 vole and soybean data sets (Figure 5B). In addition, VirID provided a more precise
482 classification system for the target viruses. For instance, viruses that were previously classified
483 only at the kingdom level, such as Bulatov virus, Fennes virus, Ronne virus, and Vovk virus
484 from the seabird tick data set, were now classified at the genus level (Supplementary Table S7).

485 VirID also provides information on whether the viruses observed are associated with
486 vertebrates, plants, or have the potential to infect humans. For example, in the Qinghai vole
487 data set we identified 180 species that were likely associated with voles, including
488 *Mamastrovirus* (N = 1), *Hepacivirus* (*N = 5*), *Pegivirus* (*N = 2*), *Arteriviridae* (*N = 1*), and
489 *Picobirnaviridae* (*N =164*), although the host association for the *Picobirnaviridae* remains
490 uncertain (Sadiq, et al. 2024). Additionally, 250 virus species were likely associated with food
491 sources, parasites, and symbionts within these hosts, including Narna-Levi (*N = 163*), Partiti-
492 Picobirna (*N = 74*) and Toti-Chryso (*N = 6*) (Figure 6A). Overall, vertebrate-associated viruses
493 accounted for a median of 66% of the total non-ribosomal RNA in host samples, ranging from
494 30.2-73.6%, while other viruses accounted for 23.3%, with a range of 10.5-67.9% (Figure 6B).
495 Notably, we identified two species, Hepatovirus D and Rotavirus A, that are potential human
496 pathogens. Hepatovirus D was described in the original publication (He, Wang, et al. 2022),
497 while Rotavirus A was newly identified here. These viruses were discovered because they
498 cluster with known human pathogens at over 80% sequence identity with these viral contigs.
499 Similarly, we identified 17 potential human pathogens, primarily within the clinical sample
500 data set. This included potential human pathogens such as Pangolin coronavirus HKU4,
501 Rotavirus A, and Pangolin Respirovirus identified in pangolins, as well as the vector-borne
502 Gadgets Gully virus, Okhotskiy virus, and Neke harbour virus from the seabird tick samples.
503 This is consistent with previous publications. Additionally, plant-infecting viruses were
504 identified in the vole (*N = 5*, likely diet-related), soybean (*N = 6*), and soil (*N = 24*) samples
505 (Figure 6C, Supplementary Table S8). In the Soybean field data set, we detected 79 contigs
506 from six viral species associated with plants, constituting about 74.5% of the total non-
507 ribosomal RNA, including tobacco streak virus, soybean dwarf virus, pepper mild mottle virus,
508 bean pod mottle virus, and alfalfa mosaic virus (Figure 6D).
509
510 **Discussion**
511 Herein, we present VirID, an RNA virus discovery platform specifically designed for
512 Linux servers. VirID integrates phylogenetic analysis into the identification and
513 characterization of RNA viruses, thereby substantially improving virus discovery. The platform

514 employs an iterative scoring strategy in its alignment processes to minimize false positives and
515 incorporates a phylogenetic placement algorithm for the rapid and stable phylogenetic tree
516 inference. As a result, users can accurately estimate RNA virus diversity, classify each
517 identified virus with high precision, at the same time obtaining insights into host associations
518 which enable the potential threat to human, animal and plant health to be evaluated. The wealth
519 of information generated by this platform will be invaluable for researchers involved in early
520 warning of infectious diseases across diverse settings.

521 Our results show that VirID provides the most precise estimation of viral species
522 composition, while other programs tend to overestimate genetic diversity. This overestimation
523 may occur because some methods consider all virus-associated contigs, including those with
524 low coverage and fragmented genomes, potentially counting them as multiple species. To
525 depict diversity more accurately, it is essential to focus on regions of the genome shared by the
526 majority of viruses, thereby minimizing overestimation (Beerenwinkel, et al. 2012; García-
527 López, et al. 2015). The RdRP gene is an excellent candidate for several reasons. First, all RNA
528 viruses, with the exception of RNA satellite viruses, contain the RdRP (Shi, et al. 2016; Shi,
529 Lin, et al. 2018; Zayed, et al. 2022). Second, the RdRP protein is the most conserved gene in
530 the RNA virus genome, and often comparable across different virus classes or even phyla
531 (Venkataraman, et al. 2018; Mönttinen, et al. 2021). Therefore, focusing solely on RdRP
532 contigs is key to accurately determining viral diversity within a sample.

533 Compared to other virus discovery programs, the phylogenetic analysis feature of VirID
534 provides a central analytical component. In particular, it provides an automated and reliable
535 method for accurately classifying previously undescribed RNA viruses, especially those that
536 are highly divergent in sequence. Traditionally, the approach to classifying new viruses
537 involved BLAST analyses and assigning taxonomic position based on the closest related hits
538 (Lin, et al. 2017; Zhao, et al. 2017; Plyusnin, et al. 2023). However, this method may counter
539 the guidelines laid down by the International Committee on Taxonomy of Viruses (ICTV) who
540 apply varying criteria for virus taxonomy at the species and genus levels (King, et al. 2012;
541 Simmonds, et al. 2017; Lefkowitz, et al. 2018). Additionally, the lack of a clear definition of
542 what levels of genetic similarity differentiate higher taxonomic ranks complicates the

543 assignment of viruses to new families or orders when protein identity is below 40%. More
544 importantly, some reference sequences are incorrectly classified, which can introduce errors
545 into the classification process. For instance, a sequence from soil metagenomic data
546 (MN035928), from a divergent member within the order *Bunyavirales*, was mistakenly labeled
547 as belonging to the genus *Arenavirus* within the *Arenaviridae* (Starr, et al. 2019). As a
548 consequence, subsequent discoveries of similar viruses (OQ715420)(Chen, Hu, et al. 2023)
549 were also mislabeled as *Arenaviridae*. Such misclassifications could be avoided with robust
550 and reliable phylogenetic analyses.

551 Phylogenetic analysis is also central to the inference of host associations. Viruses from
552 similar host categories tend to cluster together, forming what is known as a phylogenetic
553 monophyly, indicative of host structure in virus phylogeny (Kitchen, et al. 2011; Shi, et al.
554 2016; Shi, Lin, et al. 2018; French, et al. 2023). This pattern holds true across different types
555 of viruses, such as vertebrate-specific viruses, arthropod-borne viruses, and plant viruses, in
556 which host-associated phylogenetic monophyletic groups are identifiable at various taxonomic
557 levels—ranging from the family level (e.g., *Picornaviridae*) to the genus level (e.g.,
558 *Alphavirus*), and even within specific genetic lineages in a single genus (e.g., mosquito-borne
559 and tick-borne virus groups within genus *Flavivirus*). Due to the varying scales and complexity
560 of these host-associated groups, phylogenetic analysis serves as a valuable tool for exploring
561 these relationships (Shi, et al. 2022; Cui, et al. 2023; Wang, et al. 2023). However, assigning
562 viruses to other host groups such as arthropods, nematodes, and even basal eukaryotes (such
563 as parasites) remains challenging due to the scarcity of relevant virus data on these hosts. In
564 addition, a limitation to all virus discovery tools, including VirID, is that they may not identify
565 vertebrate-associated viruses if they occupy phylogenetic positions not previously linked to
566 vertebrate hosts.

567 The ability to infer host associations is highly relevant in disease monitoring programs in
568 which emerging pathogens are continuously identified and evaluated (Carroll, et al. 2018;
569 Carlson, et al. 2022; Ko, et al. 2022). Numerous viruses are discovered in sequencing efforts,
570 but not all are relevant to the infection of principal host or impact health. Indeed, those relevant
571 to disease often constitute only a small fraction (Liang and Bushman 2021). For example, in a

572 survey of over 1941 game animals across China, more than 1000 viruses were identified, yet
573 only 102 were linked to mammalian infections, and even fewer (N = 21) were considered to
574 pose a significant risk of infecting humans or other animal species (He, Hou, et al. 2022).
575 Similarly, a recent meta-transcriptomics study of 2438 mosquitoes in China revealed that
576 among the 564 RNA virus species detected, 393 were likely associated with mosquitoes, but
577 only 7 were linked to mammalian infections (i.e., arboviruses) (Pan, et al. 2024). Thus,
578 discerning potential host associations is crucial for assessing the public health or economic
579 impact of discovered viruses (Rahman, et al. 2020; Bernstein, et al. 2022; Lefrançois, et al.
580 2023).

581 Our study is subject to several limitations. First, while the phylogenetic placement method
582 has accelerated the estimation of evolutionary trees, the self-iterative multi-sequence alignment
583 process remains time-consuming. Second, VirID primarily relies on the RdRP to denote
584 homology and is therefore unable to identify sequences that do not contain RdRP sequences or
585 that are too divergent to be detected in homology-based searches (Telesnitsky and Goff 2011;
586 Hu and Hughes 2012). Consequently, for segmented viruses, the full genome assembly may be
587 incomplete. Third, VirID does not provide strain or genotype level typing which often depend
588 on more variable parts of viral genomes (Yang, et al. 2020; Liao, et al. 2022). Finally, the RdRP
589 database is continuously expanding, particularly with the addition of data from environmental
590 samples (Wolf, et al. 2020; Chen, et al. 2022; Edgar, et al. 2022; Zayed, et al. 2022; Hou, et al.
591 2023). However, since these environmental RdRP data are unverified, and this study focuses
592 on human, animal, and plant health, they are currently excluded from our database.
593 Nevertheless, given the flexibility of our RdRP database structure, these data can be readily
594 incorporated to facilitate future broader scale analyses.
595

596 **Data Availability**

597 VirID is freely available as an open-source Python code at
598 https://github.com/ZiyueYang01/VirID. And the newly identified virus sequences from this
599 study are available under the link:
600 https://github.com/ZiyueYang01/VirID/blob/main/data_res/Novel_RNA_viral.fasta

Supplementary Data

Supplementary Data are available at MBE Online.

Author Contributions

Conceptualization, EC Holmes, DY Guo and M Shi; Methodology, ZY Yang, YT Shan, X Liu, GW Chen, YF Pan, DY Guo and M Shi; Investigation, ZY Yang and YT Shan; Data Collection and Processing, QY Gou, J Zou, ZL Chang, Q Zeng, CH Yang, JB Kong, WC Wu, DY Guo and M Shi; Writing – Original Draft, ZY Yang and YT Shan; Writing – Review and Editing, All authors. Funding Acquisition, CM Li, H Peng, DY Guo and M Shi; Resources (computational), SC Li, X Zhang, DY Guo and M Shi; Supervision, CM Li, H Peng, DY Guo and M Shi.

Funding

This study is funded by National Natural Science Foundation of China (82341118, 32270160), Natural Science Foundation of Guangdong Province of China (2022A1515011854), Shenzhen Science and Technology Program (JCYJ20210324124414040, KQTD20200820145822023), Hong Kong Innovation and Technology Fund (ITF) (MRP/071/20X), Major Project of Guangzhou National Laboratory (GZNL2023A01001), Guangdong Province "Pearl River Talent Plan" Innovation, Entrepreneurship Team Project (2019ZT08Y464), and the Fund of Shenzhen Key Laboratory (ZDSYS20220606100803007). E.C. Holmes was supported by an NHMRC (Australia) Investigator Award (GNT2017197) and by AIR@InnoHK administered by the Innovation and Technology Commission, Hong Kong Special Administrative Region, China.

References

Abascal F, Zardoya R, Posada D. 2005. ProtTest: selection of best-fit models of protein evolution. Bioinformatics 21:2104-2105.

Akhter S, Aziz RK, Edwards RA. 2012. PhiSpy: a novel algorithm for finding prophages in bacterial genomes that combines similarity-and composition-based strategies. Nucleic acids research 40:e126-e126.

632 Allaire J, Ellis P, Gandrud C, Kuo K, Lewis B, Owen J, Russell K, Rogers J, Sese C, Yetman
633 C. 2017. Package 'networkD3'. D3 JavaScript network graphs from R.

634 Assiri A, McGeer A, Perl TM, Price CS, Al Rabeeah AA, Cummings DA, Alabdullatif ZN,
635 Assad M, Almulhim A, Makhdoom H. 2013. Hospital outbreak of Middle East respiratory
636 syndrome coronavirus. New England Journal of Medicine 369:407-416.

637 Babaian A, Edgar R. 2022. Ribovirus classification by a polymerase barcode sequence. PeerJ
638 10:e14055.

639 Beerenwinkel N, Günthard HF, Roth V, Metzner KJ. 2012. Challenges and opportunities in
640 estimating viral genetic diversity from next-generation sequencing data. Frontiers in
641 microbiology 3:31515.

642 Bender KM, Svenning MM, Hu Y, Richter A, Schückel J, Jørgensen B, Liebner S, Tveit AT.
643 2021. Microbial responses to herbivory-induced vegetation changes in a high-Arctic peatland.
644 Polar Biology 44:899-911.

645 Bernstein AS, Ando AW, Loch-Temzelides T, Vale MM, Li BV, Li H, Busch J, Chapman CA,
646 Kinnaird M, Nowak K. 2022. The costs and benefits of primary prevention of zoonotic
647 pandemics. Science Advances 8:eabl4183.

648 Buchfink B, Xie C, Huson DH. 2015. Fast and sensitive protein alignment using DIAMOND.
649 Nature methods 12:59-60.

650 Bushnell B. 2014. BBMap: a fast, accurate, splice-aware aligner. In: Lawrence Berkeley
651 National Lab.(LBNL), Berkeley, CA (United States).

652 Camacho C, Coulouris G, Avagyan V, Ma N, Papadopoulos J, Bealer K, Madden TL. 2009.
653 BLAST+: architecture and applications. BMC bioinformatics 10:1-9.

654 Capella-Gutiérrez S, Silla-Martínez JM, Gabaldón T. 2009. trimAl: a tool for automated
655 alignment trimming in large-scale phylogenetic analyses. Bioinformatics 25:1972-1973.

656 Carlson CJ, Albery GF, Merow C, Trisos CH, Zipfel CM, Eskew EA, Olival KJ, Ross N,
657 Bansal S. 2022. Climate change increases cross-species viral transmission risk. Nature
658 607:555-562.

659 Carroll D, Daszak P, Wolfe ND, Gao GF, Morel CM, Morzaria S, Pablos-Méndez A, Tomori
660 O, Mazet JA. 2018. The global virome project. Science 359:872-874.

661 Chan JF-W, To KK-W, Tse H, Jin D-Y, Yuen K-Y. 2013. Interspecies transmission and
662 emergence of novel viruses: lessons from bats and birds. Trends in microbiology 21:544-555.

663 Chang W-S, Eden J-S, Hall J, Shi M, Rose K, Holmes EC. 2020. Metatranscriptomic analysis
664 of virus diversity in urban wild birds with paretic disease. Journal of Virology 94:10.1128/jvi.
665 00606-00620.

666 Chen G, Tang X, Shi M, Sun Y. 2023. VirBot: an RNA viral contig detector for metagenomic
667 data. Bioinformatics 39:btad093.

668 Chen Y-M, Hu S-J, Lin X-D, Tian J-H, Lv J-X, Wang M-R, Luo X-Q, Pei Y-Y, Hu R-X, Song
669 Z-G. 2023. Host traits shape virome composition and virus transmission in wild small
670 mammals. Cell 186:4662-4675. e4612.

671 Chen Y-M, Sadiq S, Tian J-H, Chen X, Lin X-D, Shen J-J, Chen H, Hao Z-Y, Wille M, Zhou
672 Z-C. 2022. RNA viromes from terrestrial sites across China expand environmental viral
673 diversity. Nature Microbiology 7:1312-1323.

674 Claas EC, Osterhaus AD, Van Beek R, De Jong JC, Rimmelzwaan GF, Senne DA, Krauss S,
675 Shortridge KF, Webster RG. 1998. Human influenza A H5N1 virus related to a highly
676 pathogenic avian influenza virus. The Lancet 351:472-477.

677 Cole JR, Chai B, Farris RJ, Wang Q, Kulam-Syed-Mohideen A, McGarrell DM, Bandela A,
678 Cardenas E, Garrity GM, Tiedje JM. 2007. The ribosomal database project (RDP-II):
679 introducing myRDP space and quality controlled public data. Nucleic acids research
680 35:D169-D172.

681 Cui X, Fan K, Liang X, Gong W, Chen W, He B, Chen X, Wang H, Wang X, Zhang P. 2023.
682 Virus diversity, wildlife-domestic animal circulation and potential zoonotic viruses of small
683 mammals, pangolins and zoo animals. Nature Communications 14:2488.

684 Culley AI, Lang AS, Suttle CA. 2003. High diversity of unknown picorna-like viruses in the
685 sea. Nature 424:1054-1057.

686 Drake JW. 1993. Rates of spontaneous mutation among RNA viruses. Proceedings of the
687 National Academy of Sciences 90:4171-4175.

688 Dutilh BE, Varsani A, Tong Y, Simmonds P, Sabanadzovic S, Rubino L, Roux S, Munoz AR,
689 Lood C, Lefkowitz EJJCoiv. 2021. Perspective on taxonomic classification of uncultivated
690 viruses. 51:207-215.

691 Edgar RC, Taylor B, Lin V, Altman T, Barbera P, Meleshko D, Lohr D, Novakovsky G,
692 Buchfink B, Al-Shayeb B. 2022. Petabase-scale sequence alignment catalyses viral discovery.
693 Nature 602:142-147.

694 Elmore MG, Groves CL, Hajimorad M, Stewart TP, Gaskill MA, Wise KA, Sikora E,
695 Kleczewski NM, Smith DL, Mueller DS. 2022. Detection and discovery of plant viruses in
696 soybean by metagenomic sequencing. Virology journal 19:149.

697 Ergönül Ö. 2006. Crimean-Congo haemorrhagic fever. The Lancet Infectious Diseases 6:203-
698 214.

699 Fauci AS. 1988. The human immunodeficiency virus: infectivity and mechanisms of
700 pathogenesis. Science 239:617-622.

701 Feng Y, Gou Q-y, Yang W-h, Wu W-c, Wang J, Holmes EC, Liang G, Shi M. 2022. A time-
702 series meta-transcriptomic analysis reveals the seasonal, host, and gender structure of
703 mosquito viromes. Virus Evolution 8:veac006.

704 Flygare S, Simmon K, Miller C, Qiao Y, Kennedy B, Di Sera T, Graf EH, Tardif KD, Kapusta
705 A, Rynearson S. 2016. Taxonomer: an interactive metagenomics analysis portal for universal
706 pathogen detection and host mRNA expression profiling. Genome biology 17:1-18.

707 French RK, Anderson SH, Cain KE, Greene TC, Minor M, Miskelly CM, Montoya JM, Wille
708 M, Muller CG, Taylor MW. 2023. Host phylogeny shapes viral transmission networks in an
709 island ecosystem. Nature Ecology & Evolution 7:1834-1843.

710 Fritz A, Hofmann P, Majda S, Dahms E, Dröge J, Fiedler J, Lesker TR, Belmann P, DeMaere
711 MZ, Darling AE. 2019. CAMISIM: simulating metagenomes and microbial communities.
712 Microbiome 7:1-12.

713 Fu L, Niu B, Zhu Z, Wu S, Li W. 2012. CD-HIT: accelerated for clustering the next-
714 generation sequencing data. Bioinformatics 28:3150-3152.

715 García-López R, Vázquez-Castellanos JF, Moya A. 2015. Fragmentation and coverage
716 variation in viral metagenome assemblies, and their effect in diversity calculations. Frontiers
717 in bioengineering and biotechnology 3:141.

718 Graf EH, Simmon KE, Tardif KD, Hymas W, Flygare S, Eilbeck K, Yandell M, Schlaberg R.
719 2016. Unbiased detection of respiratory viruses by use of RNA sequencing-based
720 metagenomics: a systematic comparison to a commercial PCR panel. Journal of clinical
721 microbiology 54:1000-1007.

722 Greninger AL. 2018. A decade of RNA virus metagenomics is (not) enough. Virus research
723 244:218-229.

724 Guo J, Bolduc B, Zayed AA, Varsani A, Dominguez-Huerta G, Delmont TO, Pratama AA,
725 Gazitúa MC, Vik D, Sullivan MB. 2021. VirSorter2: a multi-classifier, expert-guided
726 approach to detect diverse DNA and RNA viruses. Microbiome 9:1-13.

727 He S, Krainer KMC. 2020. Pandemics of people and plants: which is the greater threat to
728 food security? Molecular plant 13:933-934.

729 He W-T, Hou X, Zhao J, Sun J, He H, Si W, Wang J, Jiang Z, Yan Z, Xing G. 2022. Virome
730 characterization of game animals in China reveals a spectrum of emerging pathogens. Cell
731 185:1117-1129. e1118.

732 He X, Wang X, Fan G, Li F, Wu W, Wang Z, Fu M, Wei X, Ma S, Ma X. 2022. Metagenomic
733 analysis of viromes in tissues of wild Qinghai vole from the eastern Tibetan Plateau.
734 Scientific Reports 12:17239.

735 Hegarty B, Riddell V J, Bastien E, Langenfeld K, Lindback M, Saini JS, Wing A, Zhang J,
736 Duhaime MJM. 2024. Benchmarking informatics approaches for virus discovery: caution is
737 needed when combining in silico identification methods. 9:e01105-01123.

738 Holmes EC. 2009. The evolution and emergence of RNA viruses: Oxford University Press.

739 Hou X, He Y, Fang P, Mei S-Q, Xu Z, Wu W-C, Tian J-H, Zhang S, Zeng Z-Y, Gou Q-Y.

740 2023. Artificial intelligence redefines RNA virus discovery. bioRxiv:2023.2004.
741 2018.537342.

742 Hu W-S, Hughes SH. 2012. HIV-1 reverse transcription. Cold Spring Harbor Perspectives in
743 Medicine 2:a006882.

744 Huhtamo E, Moureau G, Cook S, Julkunen O, Putkuri N, Kurkela S, Uzcategui NY, Harbach
745 RE, Gould EA, Vapalahti O. 2012. Novel insect-specific flavivirus isolated from northern
746 Europe. Virology 433:471-478.

747 Hunter JD. 2007. Matplotlib: A 2D graphics environment. Computing in science &
748 engineering 9:90-95.

749 Kalantar KL, Carvalho T, de Bourcy CF, Dimitrov B, Dingle G, Egger R, Han J, Holmes OB,
750 Juan Y-F, King R. 2020. IDseq—An open source cloud-based pipeline and analysis service
751 for metagenomic pathogen detection and monitoring. Gigascience 9:giaa111.

752 Katoh K, Standley DM. 2013. MAFFT multiple sequence alignment software version 7:
753 improvements in performance and usability. Molecular biology and evolution 30:772-780.

754 Kieft K, Zhou Z, Anantharaman K. 2020. VIBRANT: automated recovery, annotation and
755 curation of microbial viruses, and evaluation of viral community function from genomic
756 sequences. Microbiome 8:1-23.

757 King AM, Adams MJ, Carstens EB, Lefkowitz EJ. 2012. Virus taxonomy. Ninth report of the
758 International Committee on Taxonomy of Viruses 9.

759 Kitchen A, Shackelton LA, Holmes EC. 2011. Family level phylogenies reveal modes of
760 macroevolution in RNA viruses. Proceedings of the National Academy of Sciences 108:238-
761 243.

762 Ko KK, Chng KR, Nagarajan N. 2022. Metagenomics-enabled microbial surveillance. Nature
763 Microbiology 7:486-496.

764 Lam TT-Y, Jia N, Zhang Y-W, Shum MH-H, Jiang J-F, Zhu H-C, Tong Y-G, Shi Y-X, Ni X-B,
765 Liao Y-S. 2020. Identifying SARS-CoV-2-related coronaviruses in Malayan pangolins.
766 Nature 583:282-285.

767 Langmead B, Salzberg SL. 2012. Fast gapped-read alignment with Bowtie 2. Nature methods
768 9:357-359.

769 Lee C. 2015. Porcine epidemic diarrhea virus: an emerging and re-emerging epizootic swine
770 virus. Virology Journal 12:1-16.

771 Lefkowitz EJ, Dempsey DM, Hendrickson RC, Orton RJ, Siddell SG, Smith DB. 2018. Virus
772 taxonomy: the database of the International Committee on Taxonomy of Viruses (ICTV).
773 Nucleic acids research 46:D708-D717.

774 Lefrançois T, Malvy D, Atlani-Duault L, Benamouzig D, Druais P-L, Yazdanpanah Y,
775 Delfraissy J-F, Lina B. 2023. After 2 years of the COVID-19 pandemic, translating One

776 Health into action is urgent. The Lancet 401:789-794.

777 Li C-X, Shi M, Tian J-H, Lin X-D, Kang Y-J, Chen L-J, Qin X-C, Xu J, Holmes EC, Zhang
778 Y-Z. 2015. Unprecedented genomic diversity of RNA viruses in arthropods reveals the
779 ancestry of negative-sense RNA viruses. elife 4:e05378.

780 Li D, Liu C-M, Luo R, Sadakane K, Lam T-W. 2015. MEGAHIT: an ultra-fast single-node
781 solution for large and complex metagenomics assembly via succinct de Bruijn graph.
782 Bioinformatics 31:1674-1676.

783 Liang G, Bushman FD. 2021. The human virome: assembly, composition and host
784 interactions. Nature Reviews Microbiology 19:514-527.

785 Liao H, Cai D, Sun Y. 2022. VirStrain: a strain identification tool for RNA viruses. Genome
786 biology 23:38.

787 Lin J, Kramna L, Autio R, Hyöty H, Nykter M, Cinek O. 2017. Vipie: web pipeline for
788 parallel characterization of viral populations from multiple NGS samples. Bmc Genomics
789 18:1-11.

790 Mackenzie JS, Gubler DJ, Petersen LR. 2004. Emerging flaviviruses: the spread and
791 resurgence of Japanese encephalitis, West Nile and dengue viruses. Nature medicine 10:S98-
792 S109.

793 Martina BE, Koraka P, Osterhaus AD. 2009. Dengue virus pathogenesis: an integrated view.
794 Clinical microbiology reviews 22:564-581.

795 Matsen FA, Kodner RB, Armbrust EV. 2010. pplacer: linear time maximum-likelihood and
796 Bayesian phylogenetic placement of sequences onto a fixed reference tree. BMC
797 bioinformatics 11:1-16.

798 Mifsud JC, Gallagher RV, Holmes EC, Geoghegan JL. 2022. Transcriptome mining expands
799 knowledge of RNA viruses across the plant kingdom. Journal of Virology 96:e00260-00222.

800 Mihara T, Nishimura Y, Shimizu Y, Nishiyama H, Yoshikawa G, Uehara H, Hingamp P, Goto
801 S, Ogata H. 2016. Linking virus genomes with host taxonomy. Viruses 8:66.

802 Mönttinen HA, Ravantti JJ, Poranen MM. 2021. Structure unveils relationships between
803 RNA virus polymerases. Viruses 13:313.

804 Musso D, Gubler DJ. 2016. Zika virus. Clinical microbiology reviews 29:487-524.

805 Nayfach S, Camargo AP, Schulz F, Eloe-Fadrosh E, Roux S, Kyrpides NC. 2021. CheckV
806 assesses the quality and completeness of metagenome-assembled viral genomes. Nature
807 biotechnology 39:578-585.

808 Nicaise V. 2014. Crop immunity against viruses: outcomes and future challenges. Frontiers in
809 plant science 5:660.

810 Pan Y-F, Zhao H, Gou Q-Y, Shi P-B, Tian J-H, Feng Y, Li K, Yang W-H, Wu D, Tang G.

2024. Metagenomic analysis of individual mosquito viromes reveals the geographical patterns and drivers of viral diversity. Nature Ecology & Evolution 8:947-959.

Peiris JM, De Jong MD, Guan Y. 2007. Avian influenza virus (H5N1): a threat to human health. Clinical microbiology reviews 20:243-267.

Pettersson JH-O, Ellström P, Ling J, Nilsson I, Bergström S, González-Acuña D, Olsen B, Holmes EC. 2020. Circumpolar diversification of the Ixodes uriae tick virome. PLoS Pathogens 16:e1008759.

Plyusnin I, Vapalahti O, Sironen T, Kant R, Smura T. 2023. Enhanced viral metagenomics with lazypipe 2. Viruses 15:431.

Quast C, Pruesse E, Yilmaz P, Gerken J, Schweer T, Yarza P, Peplies J, Glöckner FO. 2012. The SILVA ribosomal RNA gene database project: improved data processing and web-based tools. Nucleic acids research 41:D590-D596.

Rahman MT, Sobur MA, Islam MS, Ievy S, Hossain MJ, El Zowalaty ME, Rahman AT, Ashour HM. 2020. Zoonotic diseases: etiology, impact, and control. Microorganisms 8:1405.

Rampelli S, Soverini M, Turroni S, Quercia S, Biagi E, Brigidi P, Candela M. 2016. ViromeScan: a new tool for metagenomic viral community profiling. Bmc Genomics 17:1-9.

Ren J, Ahlgren NA, Lu YY, Fuhrman JA, Sun F. 2017. VirFinder: a novel k-mer based tool for identifying viral sequences from assembled metagenomic data. Microbiome 5:1-20.

Ren J, Song K, Deng C, Ahlgren NA, Fuhrman JA, Li Y, Xie X, Poplin R, Sun F. 2020. Identifying viruses from metagenomic data using deep learning. Quantitative Biology 8:64-77.

Robilotti E, Deresinski S, Pinsky BA. 2015. Norovirus. Clinical microbiology reviews 28:134-164.

Roux S, Enault F, Hurwitz BL, Sullivan MB. 2015. VirSorter: mining viral signal from microbial genomic data. PeerJ 3:e985.

Sadiq S, Holmes EC, Mahar JE. 2024. Genomic and phylogenetic features of the Picobirnaviridae suggest microbial rather than animal hosts. Virus Evolution 10:veae033.

Scholthof KBG, Adkins S, Czosnek H, Palukaitis P, Jacquot E, Hohn T, Hohn B, Saunders K, Candresse T, Ahlquist P. 2011. Top 10 plant viruses in molecular plant pathology. Molecular plant pathology 12:938-954.

Shen W, Ren H. 2021. TaxonKit: A practical and efficient NCBI taxonomy toolkit. Journal of Genetics and Genomics 48:844-850.

Shi M, Hou X, He Y, Fang P, Mei S-Q, Xu Z, Wu W-C, Tian J-h, Zhang S, Zeng Z-Y. 2023. Artificial intelligence redefines RNA virus discovery.

Shi M, Lin X-D, Chen X, Tian J-H, Chen L-J, Li K, Wang W, Eden J-S, Shen J-J, Liu L, et al.

2018. The evolutionary history of vertebrate RNA viruses. Nature 556:197-202.

Shi M, Lin X-D, Tian J-H, Chen L-J, Chen X, Li C-X, Qin X-C, Li J, Cao J-P, Eden J-S, et al. 2016. Redefining the invertebrate RNA virosphere. Nature 540:539-543.

Shi M, Zhang Y-Z, Holmes EC. 2018. Meta-transcriptomics and the evolutionary biology of RNA viruses. Virus Research 243:83-90.

Shi W, Shi M, Que T-C, Cui X-M, Ye R-Z, Xia L-Y, Hou X, Zheng J-J, Jia N, Xie X. 2022. Trafficked Malayan pangolins contain viral pathogens of humans. Nature Microbiology 7:1259-1269.

Simmonds P, Adams MJ, Benkő M, Breitbart M, Brister JR, Carstens EB, Davison AJ, Delwart E, Gorbalenya AE, Harrach B. 2017. Virus taxonomy in the age of metagenomics. Nature Reviews Microbiology 15:161-168.

Simon-Loriere E, Holmes EC. 2011. Why do RNA viruses recombine? Nature Reviews Microbiology 9:617-626.

Smith GJ, Vijaykrishna D, Bahl J, Lycett SJ, Worobey M, Pybus OG, Ma SK, Cheung CL, Raghwani J, Bhatt S. 2009. Origins and evolutionary genomics of the 2009 swine-origin H1N1 influenza A epidemic. Nature 459:1122-1125.

Stamatakis A, Hoover P, Rougemont J. 2008. A rapid bootstrap algorithm for the RAxML web servers. Systematic biology 57:758-771.

Starr EP, Nuccio EE, Pett-Ridge J, Banfield JF, Firestone MK. 2019. Metatranscriptomic reconstruction reveals RNA viruses with the potential to shape carbon cycling in soil. Proceedings of the National Academy of Sciences 116:25900-25908.

Team WER. 2014. Ebola virus disease in West Africa—the first 9 months of the epidemic and forward projections. New England Journal of Medicine 371:1481-1495.

Telesnitsky A, Goff S. 2011. Reverse transcriptase and the generation of retroviral DNA.

Untiveros M, Fuentes S, Salazar LF. 2007. Synergistic interaction of Sweet potato chlorotic stunt virus (Crinivirus) with carla-, cucumo-, ipomo-, and potyviruses infecting sweet potato. Plant disease 91:669-676.

Venkataraman S, Prasad BV, Selvarajan R. 2018. RNA dependent RNA polymerases: insights from structure, function and evolution. Viruses 10:76.

Wang J, Pan Y-f, Yang L-f, Yang W-h, Lv K, Luo C-m, Wang J, Kuang G-p, Wu W-c, Gou Q-y. 2023. Individual bat virome analysis reveals co-infection and spillover among bats and virus zoonotic potential. Nature Communications 14:4079.

Waskom ML. 2021. Seaborn: statistical data visualization. Journal of Open Source Software 6:3021.

Wickham H. 2011. ggplot2. Wiley interdisciplinary reviews: computational statistics 3:180-

881 185.

882 Wolf YI, Silas S, Wang Y, Wu S, Bocek M, Kazlauskas D, Krupovic M, Fire A, Dolja VV,
883 Koonin EV. 2020. Doubling of the known set of RNA viruses by metagenomic analysis of an
884 aquatic virome. Nature Microbiology 5:1262-1270.

885 Yang C-R, King C-C, Liu L-YD, Ku C-C. 2020. FluConvert and IniFlu: a suite of integrated
886 software to identify novel signatures of emerging influenza viruses with increasing risk.
887 BMC bioinformatics 21:1-14.

888 Yu G, Smith DK, Zhu H, Guan Y, Lam TTY. 2017. ggtree: an R package for visualization and
889 annotation of phylogenetic trees with their covariates and other associated data. Methods in
890 Ecology and Evolution 8:28-36.

891 Zayed AA, Wainaina JM, Dominguez-Huerta G, Pelletier E, Guo J, Mohssen M, Tian F,
892 Pratama AA, Bolduc B, Zablocki O. 2022. Cryptic and abundant marine viruses at the
893 evolutionary origins of Earth's RNA virome. Science 376:156-162.

894 Zhang Y-Z, Chen Y-M, Wang W, Qin X-C, Holmes EC. 2019. Expanding the RNA virosphere
895 by unbiased metagenomics. Annual Review of Virology 6:119-139.

896 Zhao G, Wu G, Lim ES, Droit L, Krishnamurthy S, Barouch DH, Virgin HW, Wang D. 2017.
897 VirusSeeker, a computational pipeline for virus discovery and virome composition analysis.
898 Virology 503:21-30.

899 Zhong N, Zheng B, Li Y, Poon L, Xie Z, Chan K, Li P, Tan S, Chang Q, Xie J. 2003.
900 Epidemiology and cause of severe acute respiratory syndrome (SARS) in Guangdong,
901 People's Republic of China, in February, 2003. The Lancet 362:1353-1358.

902 Zhou Z, Martin C, Kosmopoulos JC, Anantharaman K. 2023. ViWrap: A modular pipeline to
903 identify, bin, classify, and predict viral–host relationships for viruses from metagenomes.
904 Imeta 2:e118.

905 Zhu N, Zhang D, Wang W, Li X, Yang B, Song J, Zhao X, Huang B, Shi W, Lu R. 2020. A
906 novel coronavirus from patients with pneumonia in China, 2019. New England Journal of
907 Medicine 382:727-733.

908

909 **Tables and Figures Legends**

910

911 **Figure 1. Overview of the RdRP reference database.**

912 (**A**) Compilation of representative RdRP sequences into 24 RNA virus superclades, categorized

913 based on phylogenetic analysis.

914 (**B**) Alignment of viral superclades with the ICTV taxonomic system, spanning virus class,
915 order, and family levels. Numbers reflect the count of ICTV classifications mapped to each
916 RdRP superclade, with specific ICTV representative mapping details provided.
917 (**C**) The distribution of viral sequences across superclades and ICTV taxonomy, highlighting
918 551 vertebrate-related and 325 plant-related sequences.
919 (**D**) Using the *Reoviridae* as a case study, the diagram presents a phylogenetic tree in which
920 branch colors indicate taxonomy and background hues denote host association. Reference
921 sequences are clearly annotated based on their positions within the phylogenetic tree.
922
923 **Figure 2. VirID framework for identifying RNA viruses from sequencing samples.**
924 The VirID framework for automated RNA virus detection, which comprises three main stages:
925 (i) RNA virus discovery, (ii) phylogenetic analysis, and (iii) phylogeny-based virus
926 characterization. It produces outputs that include viral sequences, phylogenetic trees, and
927 comprehensive information including sequence length, best match of BLASTx comparison,
928 virus classification, and host association.
929
930 **Figure 3. Visualization of outputs from VirID.**
931 (**A**) Distribution of Reads Per Million (RPM) of potential viral sequences from SRA sample
932 SRR22936818, categorized by RdRP superclades and corresponding NCBI taxonomic ranks.
933 (**B**) The host associations of all identified virus sequences based on their placement in the
934 phylogenetic tree.
935 (**C**) A phylogenetic tree is used to distinguish different viral lineages and colour-coded by
936 taxonomic group. In this case, newly identified virus sequences in the Nido superclade are
937 highlighted in red at the end of the branches, emphasizing their significance.
938 (**D**) Complete nucleic acid sequences for detailed analysis and verification.
939 (**E**) Detailed information for each identified viral sequence, including host association,
940 genomic details, and taxonomic classification.
941
942 **Figure 4. Benchmarking of three tools for virus discovery using simulated data.**

943 (**A**) Performance of three bioinformatics tools – VirID, VirBot, and VirSorter2 – across 15
944 simulated samples, evaluating average accuracy, precision, recall, and F1 score. Error bars
945 represent standard errors. Notably, the training data sets for VirSorter2 and VirBot are
946 primarily based on all viral genomes in the NCBI RefSeq database and a curated collection of
947 viral proteomes, respectively.
948 (**B**) The three bioinformatics tools were further assessed for their specific ability to identify
949 'new RNA viruses' at various levels of classification.
950 (**C**) Effectiveness of each tool in identifying RNA virus sequences across 15 simulated samples.
951 Yellow dots represent the number of RNA virus sequences identified, while green dots indicate
952 the number of corresponding species-level taxa.
953 (**D**) Ratio of the lengths of sequences identified by VirID in various simulated data samples
954 compared to the length of the corresponding gold standard sequence. Only sequences that
955 uniquely correspond to gold standard sequences are considered.
956
957 **Figure 5. Reclassification of viruses using VirID on real-world data.**
958 (**A**) Distribution of virus species across different superclades and families identified by VirID
959 in previously published data sets, including human swabs (Graf, et al. 2016), wild birds (Chang,
960 et al. 2020), Malayan pangolins (Shi, et al. 2022), Qinghai voles (He, Wang, et al. 2022),
961 seabird ticks (Pettersson, et al. 2020), soybean fields (Elmore, et al. 2022), and soil samples
962 (Bender, et al. 2021).
963 (**B**) The utility of VirID across a broader spectrum of RNA virus families. Virus families
964 documented in the original publications are displayed on the left, while those identified in this
965 study are shown on the right.
966
967 **Figure 6. Virus-Host associations revealed by VirID.**
968 (**A**) Number of known and unknown virus sequences related to viruses of humans, vertebrates,
969 plants, and other hosts as identified by VirID in the Qinghai vole case study.
970 (**B**) Count of virus sequences associated with different hosts in various tissue and fecal samples
971 from voles identified by VirID.

(**C**) Number and taxonomy of virus sequences related to different hosts in various real-world samples identified by VirID.

(**D**) Number of virus sequences related to viruses of different hosts in a variety of real-world samples identified by VirID.

Figure 1

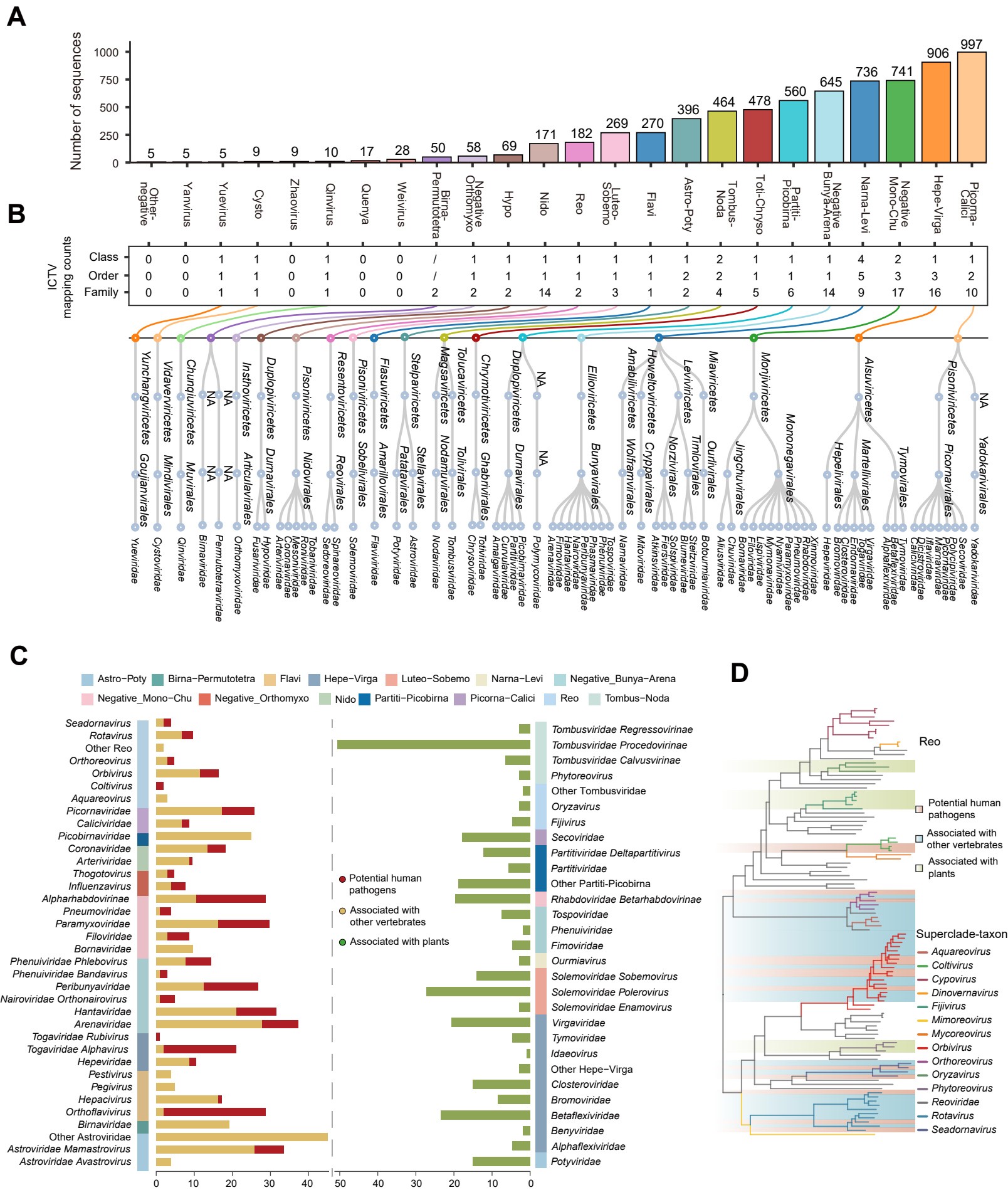
A
Number of sequences
1000
750
500
250
0
5 5 5 9 9 10 17 28 50 58 69 171 182 269 270 396 464 478 560 645 736 741 906 997
Other-negative
Yanvirus
Yuevirus
Cysto
Zhaovirus
Qinvirus
Quenya
Weivirus
Birna-Permutotetra
Negative Orthomyxo
Hypo
Nido
Reo
Luteo-Sobemo
Flavi
Astro-Poty
Tombus-Noda
Toti-Chryso
Partiti-Picobirna
Negative Bunya-Arena
Narna-Levi
Negative Mono-Chu
Hepe-Virga
Picorna-Calici
B
ICTV mapping counts
Class 0 0 1 1 0 1 0 0 / 1 1 1 1 1 1 1 2 1 1 1 4 2 1 1
Order 0 0 1 1 0 1 0 0 / 1 1 1 1 1 1 2 2 1 1 1 5 3 3 2
Family 0 0 1 1 0 1 0 0 2 2 2 14 2 3 1 2 4 5 6 14 9 17 16 10
Yunchangvirricetes
Vidaverviricetes
Chunqiuvirricetes
Insthoviricetes
Duplopiviricetes
Pisoniviricetes
Resentoviricetes
Pisoniviricetes
Flasuviricetes
Stelpaviricetes
Magsaviricetes
Tolucaviricetes
Chrymotiviricetes
Duplopiviricetes
NA
Elliioviricetes
Amabiliviricetes
Howeltoviricetes
Leviviricetes
Miaviricetes
Monjiviricetes
Alsuviricetes
Pisoniviricetes
NA
Goujianvirales
Mindivirales
Muvirales
NA
NA
Articulavirales
Durnavirales
Nidovirales
Reovirales
Sobelivirales
Amarillovirales
Patatavirales
Stellavirales
Nodamuvirales
Tolivirales
Ghabrivirales
Durnavirales
NA
Bunyavirales
Wolframvirales
Cryppavirales
Norzivirales
Timlovirales
Ourlivirales
Jingchuvirales
Mononegavirales
Hepelivirales
Martellivirales
Tymovirales
Picornavirales
Yadokarivirales
Yuevirdae
Cystoviridae
Qinviridae
Birnaviridae
Permutotetraviridae
Orthomyxoviridae
Fusariviridae
Hypoviridae
Arteriviridae
Coronaviridae
Ronniviridae
Mesoniviridae
Tobaniviridae
Spinareoviridae
Sedoreoviridae
Solemoviridae
Flaviviridae
Potyviridae
Astroviridae
Nodaviridae
Tombusviridae
Totiviridae
Chrysoviridae
Amalgaviridae
Curvulaviridae
Partitiviridae
Picobirnaviridae
Polymycoviridae
Narnaviridae
Mitoviridae
Tospoviridae
Phenuiviridae
Phasmaviridae
Nairoviridae
Hantaviridae
Fimoviridae
Arenaviridae
Xinmoviridae
Rhabdoviridae
Pneumoviridae
Paramyxoviridae
Nyamiviridae
Mymonaviridae
Lispiviridae
Filoviridae
Bornaviridae
Chuvirdae
Aliusviridae
Botourmiaviridae
Atkinsviridae
Fiersviridae
Solspiviridae
Sulemeviridae
Steitviridae
Hepeviridae
Closteroviridae
Bromoviridae
Virgaviridae
Togaviridae
Endornaviridae
Alphaflexiviridae
Betaflexiviridae
Tymoviridae
Idaeoviridae
Celiaviridae
Narnaviridae
Picornaviridae
Polycipiviridae
Secoviridae
Yadokariviridae
C
Astro−Poty
Birna−Permutotetra
Flavi
Hepe−Virga
Luteo−Sobemo
Narna−Levi
Negative_Bunya−Arena
Negative_Mono−Chu
Negative_Orthomyxo
Nido
Partiti−Picobirna
Picorna−Calici
Reo
Tombus−Noda
Seadornavirus
Rotavirus
Other Reo
Orthoreovirus
Orbivirus
Coltivirus
Aquareovirus
Picornaviridae
Caliciviridae
Picobirnaviridae
Coronaviridae
Arteriviridae
Thogotovirus
Influenzavirus
Alpharhabdovirinae
Pneumoviridae
Paramyxoviridae
Filoviridae
Bornaviridae
Phenuiviridae Phlebovirus
Phenuiviridae Bandavirus
Peribunyaviridae
Nairoviridae Orthonairovirus
Hantaviridae
Arenaviridae
Togaviridae Rubivirus
Togaviridae Alphavirus
Hepeviridae
Pestivirus
Pegivirus
Hepacivirus
Orthoflavivirus
Birnaviridae
Other Astroviridae
Astroviridae Mamastrovirus
Astroviridae Avastrovirus
0 10 20 30 40
Potential human pathogens
Associated with other vertebrates
Associated with plants
50 40 30 20 10 0
Tombusviridae Regressovirinae
Tombusviridae Procedovirinae
Tombusviridae Calvusvirinae
Phytoreovirus
Other Tombusviridae
Oryzavirus
Fijivirus
Secoviridae
Partitiviridae Deltapartitivirus
Partitiviridae
Other Partiti-Picobirna
Rhabdoviridae Betarhabdovirinae
Tospoviridae
Phenuiviridae
Fimoviridae
Ourmiavirus
Solemoviridae Sobemovirus
Solemoviridae Polerovirus
Solemoviridae Enamovirus
Virgaviridae
Tymoviridae
Idaeovirus
Other Hepe−Virga
Closteroviridae
Bromoviridae
Betaflexiviridae
Benyviridae
Alphaflexiviridae
Potyviridae
D
Reo
Potential human pathogens
Associated with other vertebrates
Associated with plants
Superclade-taxon
Aquareovirus
Coltivirus
Cypovirus
Dinovernavirus
Fijivirus
Mimoreovirus
Mycoreovirus
Orbivirus
Orthoreovirus
Oryzavirus
Phytoreovirus
Reoviridae
Rotavirus
Seadornavirus

Figure 2

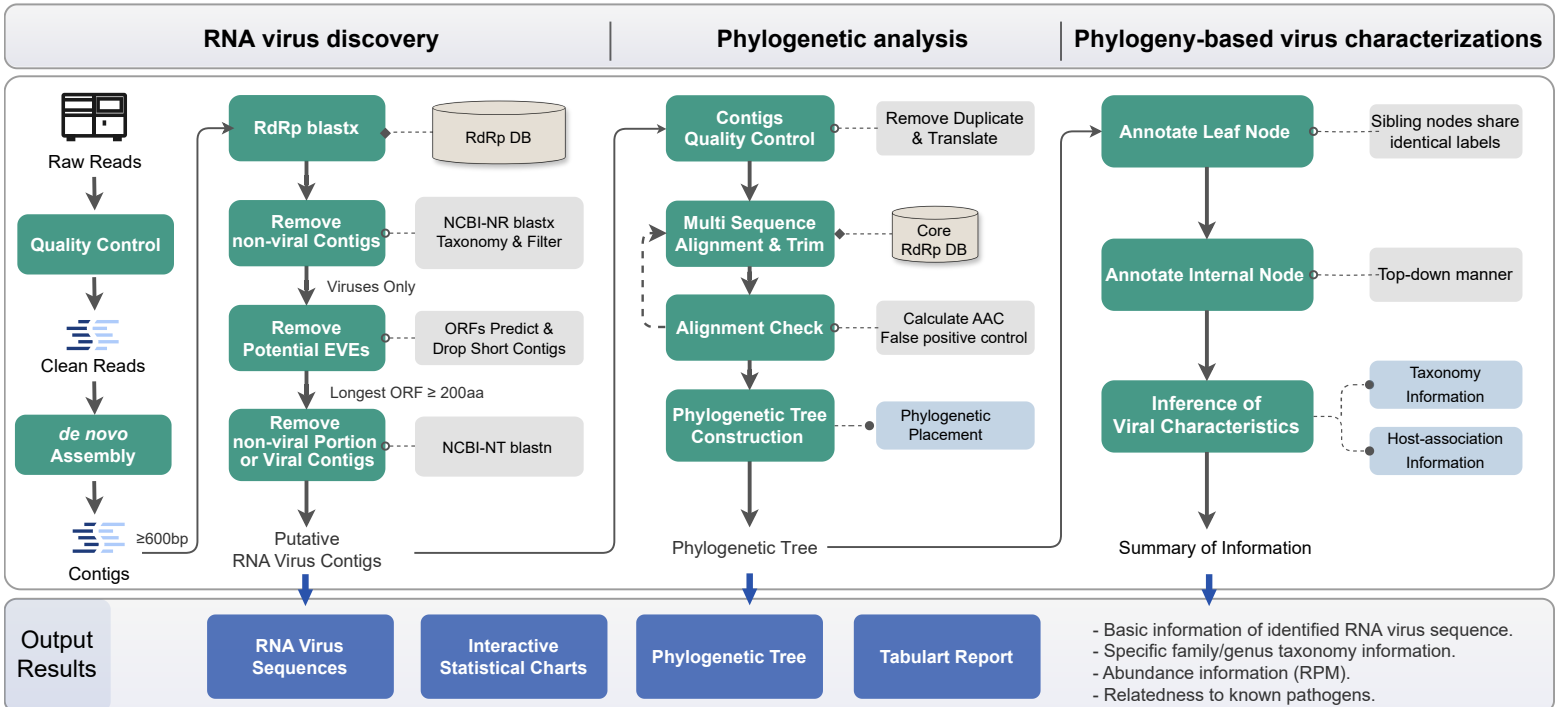
RNA virus discovery
Phylogenetic analysis
Phylogeny-based virus characterizations
Raw Reads
Quality Control
Clean Reads
de novo Assembly
≥600bp
Contigs
RdRp blastx
RdRp DB
Remove non-viral Contigs
NCBI-NR blastx Taxonomy & Filter
Viruses Only
Remove Potential EVEs
ORFs Predict & Drop Short Contigs
Longest ORF ≥ 200aa
Remove non-viral Portion or Viral Contigs
NCBI-NT blastn
Putative RNA Virus Contigs
Contigs Quality Control
Remove Duplicate & Translate
Multi Sequence Alignment & Trim
Core RdRp DB
Alignment Check
Calculate AAC False positive control
Phylogenetic Tree Construction
Phylogenetic Placement
Phylogenetic Tree
Annotate Leaf Node
Sibling nodes share identical labels
Annotate Internal Node
Top-down manner
Inference of Viral Characteristics
Taxonomy Information
Host-association Information
Summary of Information
Output Results
RNA Virus Sequences
Interactive Statistical Charts
Phylogenetic Tree
Tabulart Report
- Basic information of identified RNA virus sequence.
- Specific family/genus taxonomy information.
- Abundance information (RPM).
- Relatedness to known pathogens.

Figure 3

A. RPM plot in Sankey diagram

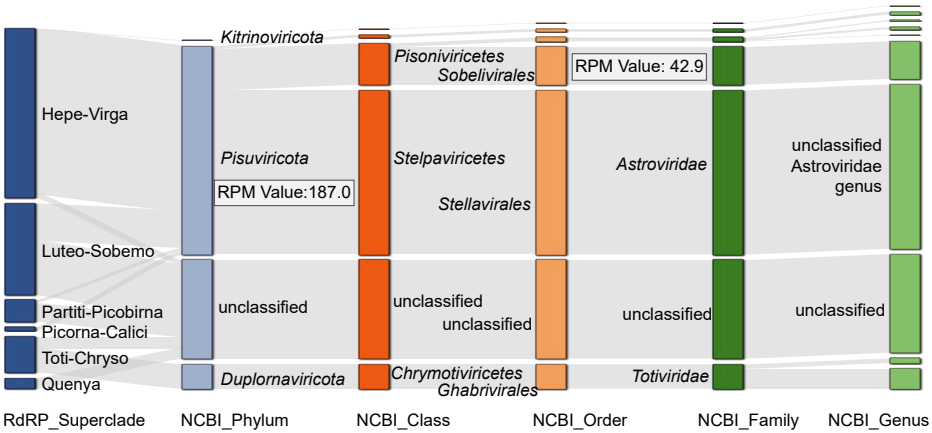

B. Distribution of likely host association

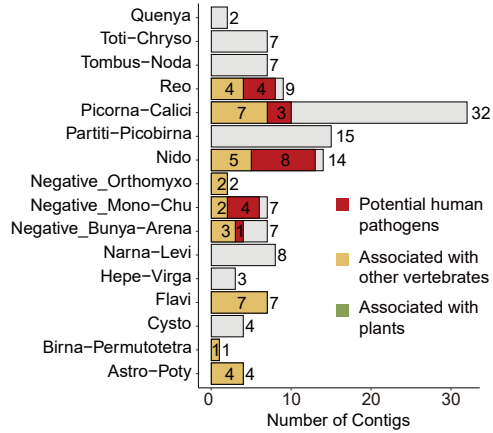

C. Phylogenetic trees at the superclade level

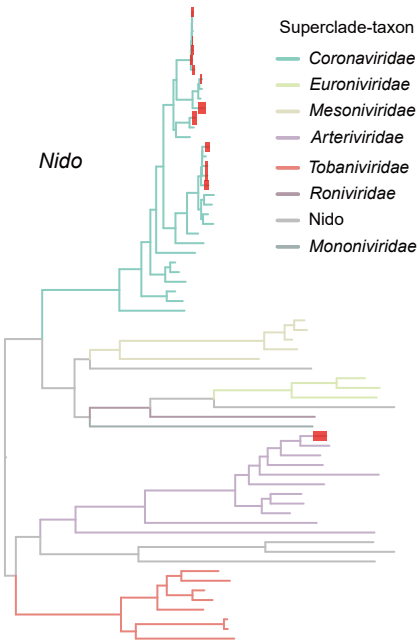

D. Nucleic acid sequence

```
>SRR22936824__k141_101227_flag_0_multi_11598.4037_len_16863
TGTCACTTACTGTACTAGCAAAGCAATATTATCGTTGCTACCGGCGTGGTCTGTATTTAAT
CCAATACGGTAGCGGTTGTATGCAGCAAAACCTGAGTCAGTGCCTACGCGCTGAGACGCTC
AATAAGAAAGCGTTCGTGAAGTAGCCACAGTGATCTCTTTTGGCAGGTCCTTGATGTCACA
GGAGTGTCCAGCCATTCGCAAGTGACCACGAATGATCACAGCACCAATGACAAGTTCACTT
```

E. Results table

SRR22936824__k141_101227_flag_0_multi_11598.4037_len_16863

qlen	Longest_aa_length	RdRP_superclade	Virus_type
16863	2628	Nido	known

Numreads	Covbases	Coverage	Meandepth
1494271	16863	100	12773.5

NR_sseqid	NR_protein
QZX47449.1	ORF1ab polyprotein

NR_Taxonomy_for_closest_hit
Viruses|Pisuviricota|Pisoniviricetes|Nidovirales|Coronaviridae|Betacoronavirus|Sarbecovirus sp.

ICTV_Taxonomy
Riboviria|Orthornavirae|Pisuviricota||Pisoniviricetes|Nidovirales|Cornidovirineae|Coronaviridae| Orthocoronavirinae|Betacoronavirus|Sarbecovirus sp.

Human	Vertebrates	Plant
1	1	0

AAI	Pathogenicity_VIRUS_FAMILY	MAX_identity	MAX_ref_id
0.590108589	*Coronaviridae*	0.949736716	NC_004718_SARS_coronavirus

Figure 4

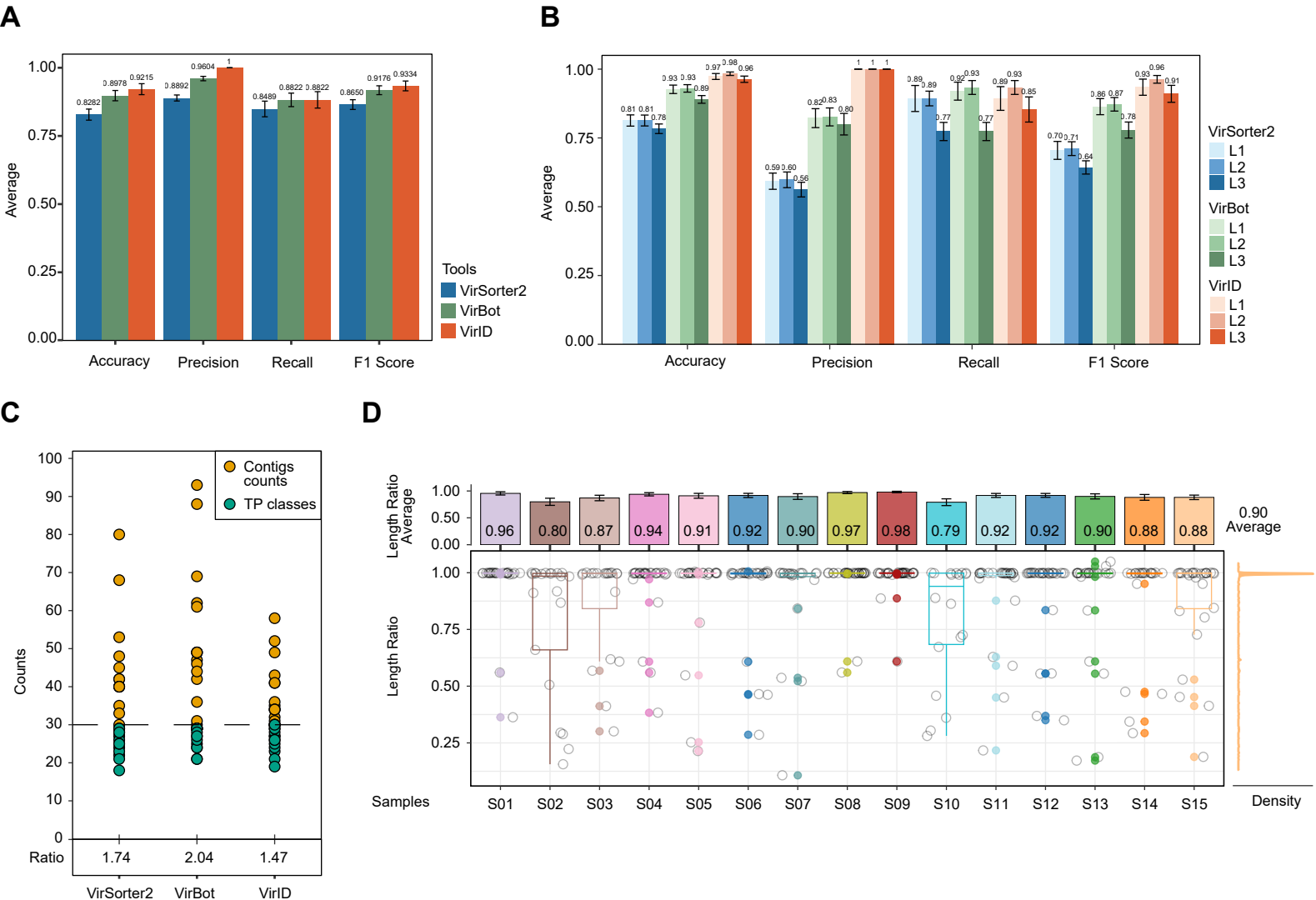
A
Average
1.00
0.75
0.50
0.25
0.00
0.8282
0.8978
0.9215
0.8892
0.9604
1
0.8489
0.8822
0.8822
0.8650
0.9176
0.9334
Accuracy
Precision
Recall
F1 Score
Tools
VirSorter2
VirBot
VirID
B
Average
1.00
0.75
0.50
0.25
0.00
0.81 0.81 0.78 0.93 0.93 0.89 0.97 0.98 0.96
0.59 0.60 0.56 0.82 0.83 0.80 1 1 1
0.89 0.89 0.77 0.92 0.93 0.77 0.89 0.93 0.85
0.70 0.71 0.64 0.86 0.87 0.78 0.93 0.96 0.91
Accuracy
Precision
Recall
F1 Score
VirSorter2
L1
L2
L3
VirBot
L1
L2
L3
VirID
L1
L2
L3
C
Counts
100
90
80
70
60
50
40
30
20
10
0
Contigs counts
TP classes
Ratio
1.74
2.04
1.47
VirSorter2
VirBot
VirID
D
Length Ratio Average
1.00
0.50
0.00
0.96 0.80 0.87 0.94 0.91 0.92 0.90 0.97 0.98 0.79 0.92 0.92 0.90 0.88 0.88
0.90 Average
Length Ratio
1.00
0.75
0.50
0.25
Samples
S01 S02 S03 S04 S05 S06 S07 S08 S09 S10 S11 S12 S13 S14 S15
Density

Figure 5

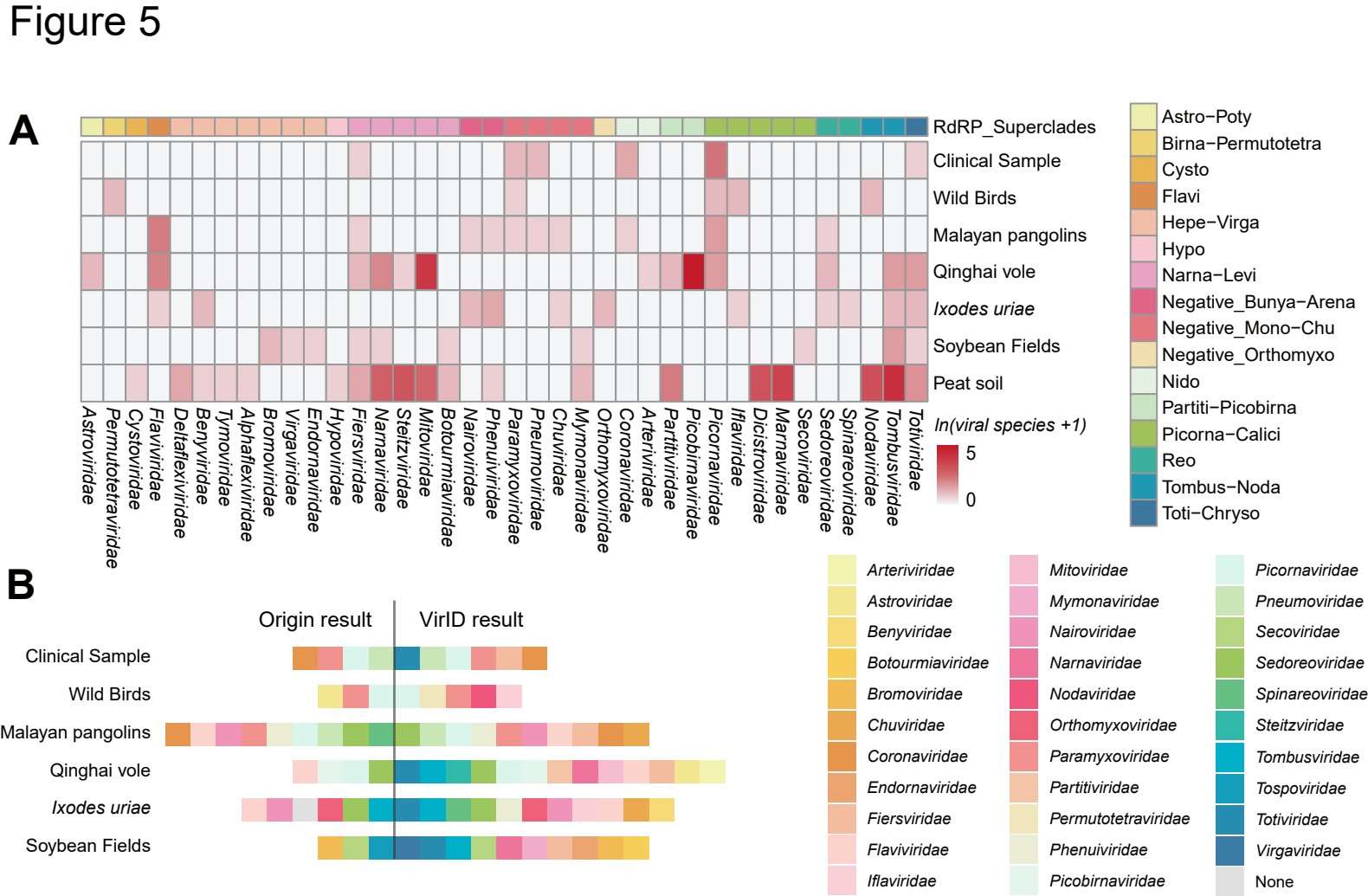
A
RdRP_Superclades
Clinical Sample
Wild Birds
Malayan pangolins
Qinghai vole
Ixodes uriae
Soybean Fields
Peat soil
Astroviridae
Permutotetraviridae
Cystoviridae
Flaviviridae
Deltaflexiviridae
Benyviridae
Tymoviridae
Alphaflexiviridae
Bromoviridae
Virgaviridae
Endornaviridae
Hypoviridae
Fiersviridae
Narnaviridae
Steitzviridae
Mitoviridae
Botourmiaviridae
Nairoviridae
Phenuiviridae
Paramyxoviridae
Pneumoviridae
Chuviridae
Mymonaviridae
Orthomyxoviridae
Coronaviridae
Arteriviridae
Partitiviridae
Picobirnaviridae
Picornaviridae
Iflaviridae
Dicistroviridae
Marnaviridae
Secoviridae
Sedoreoviridae
Spinareoviridae
Nodaviridae
Tombusviridae
Totiviridae
ln(viral species +1)
5
0
Astro−Poty
Birna−Permutotetra
Cysto
Flavi
Hepe−Virga
Hypo
Narna−Levi
Negative_Bunya−Arena
Negative_Mono−Chu
Negative_Orthomyxo
Nido
Partiti−Picobirna
Picorna−Calici
Reo
Tombus−Noda
Toti−Chryso
B
Origin result
VirID result
Clinical Sample
Wild Birds
Malayan pangolins
Qinghai vole
Ixodes uriae
Soybean Fields
Arteriviridae
Astroviridae
Benyviridae
Botourmiaviridae
Bromoviridae
Chuviridae
Coronaviridae
Endornaviridae
Fiersviridae
Flaviviridae
Iflaviridae
Mitoviridae
Mymonaviridae
Nairoviridae
Narnaviridae
Nodaviridae
Orthomyxoviridae
Paramyxoviridae
Partitiviridae
Permutotetraviridae
Phenuiviridae
Picobirnaviridae
Picornaviridae
Pneumoviridae
Secoviridae
Sedoreoviridae
Spinareoviridae
Steitzviridae
Tombusviridae
Tospoviridae
Totiviridae
Virgaviridae
None

Figure 6

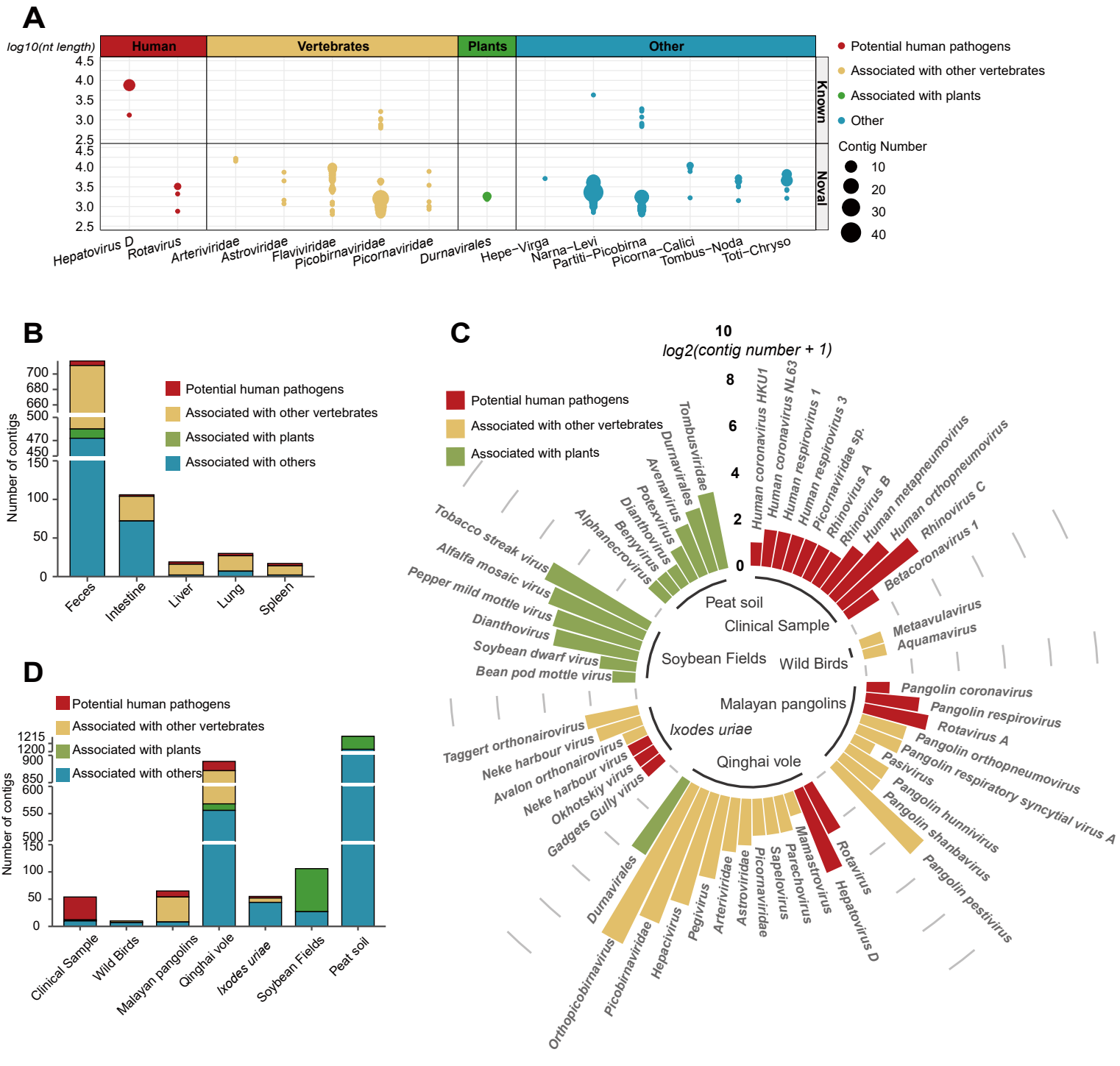
A
log10(nt length)
Human
Vertebrates
Plants
Other
Known
Novel
Potential human pathogens
Associated with other vertebrates
Associated with plants
Other
Contig Number
10
20
30
40
Hepatovirus D
Rotavirus
Arteriviridae
Astroviridae
Flaviviridae
Picobirnaviridae
Picornaviridae
Durnavirales
Hepe−Virga
Narna−Levi
Partiti−Picobirna
Picorna−Calici
Tombus−Noda
Toti−Chryso
B
Number of contigs
Potential human pathogens
Associated with other vertebrates
Associated with plants
Associated with others
Feces
Intestine
Liver
Lung
Spleen
C
log2(contig number + 1)
Potential human pathogens
Associated with other vertebrates
Associated with plants
Human coronavirus HKU1
Human coronavirus NL63
Human respirovirus 1
Human respirovirus 3
Picornaviridae sp.
Rhinovirus A
Rhinovirus B
Human metapneumovirus
Human orthopneumovirus
Rhinovirus C
Betacoronavirus 1
Metaavulavirus
Aquamavirus
Pangolin coronavirus
Pangolin respirovirus
Rotavirus A
Pangolin orthopneumovirus
Pangolin respiratory syncytial virus A
Pasivirus
Pangolin hunnivirus
Pangolin shanbavirus
Pangolin pestivirus
Rotavirus
Hepatovirus D
Mamastrovirus
Parechovirus
Sapelovirus
Picornaviridae
Astroviridae
Arteriviridae
Pegivirus
Hepacivirus
Picobirnaviridae
Orthopicobirnavirus
Durnavirales
Taggert orthonairovirus
Neke harbour virus
Avalon orthonairovirus
Neke harbour virus
Okhotskiy virus
Gadgets Gully virus
Tobacco streak virus
Alfalfa mosaic virus
Pepper mild mottle virus
Dianthovirus
Soybean dwarf virus
Bean pod mottle virus
Alphanecrovirus
Benyvirus
Dianthovirus
Potexvirus
Avenavirus
Durnavirales
Tombusviridae
Peat soil
Clinical Sample
Soybean Fields
Wild Birds
Malayan pangolins
Ixodes uriae
Qinghai vole
D
Number of contigs
Potential human pathogens
Associated with other vertebrates
Associated with plants
Associated with others
Clinical Sample
Wild Birds
Malayan pangolins
Qinghai vole
Ixodes uriae
Soybean Fields
Peat soil